Fast universal quantum control above the fault-tolerance threshold in silicon

arXiv:2108.02626 (8/2021)

Akito Noiri[1,*], Kenta Takeda[1], Takashi Nakajima[1], Takashi Kobayashi[2], Amir Sammak[3], Giordano Scappucci[4], and Seigo Tarucha[1,2,*]

Fault-tolerant quantum computers which can solve hard problems rely on quantum error correction[1]. One of the most promising error correction codes is the surface code[2], which requires universal gate fidelities exceeding the error correction threshold of 99 per cent[3]. Among many qubit platforms, only superconducting circuits[4], trapped ions[5], and nitrogen-vacancy centers in diamond[6] have delivered those requirements. Electron spin qubits in silicon[7–15] are particularly promising for a large-scale quantum computer due to their nanofabrication capability, but the two-qubit gate fidelity has been limited to 98 per cent due to the slow operation[16]. Here we demonstrate a two-qubit gate fidelity of 99.5 per cent, along with single-qubit gate fidelities of 99.8 per cent, in silicon spin qubits by fast electrical control using a micromagnet-induced gradient field and a tunable two-qubit coupling. We identify the condition of qubit rotation speed and coupling strength where we robustly achieve high-fidelity gates. We realize Deutsch-Jozsa and Grover search algorithms with high success rates using our universal gate set. Our results demonstrate the universal gate fidelity beyond the fault-tolerance threshold and pave the way for scalable silicon quantum computers.

Leon Camenzind

SPIN JC 27 / 9 / 2021

Fault tolerant spin qubits – surface code

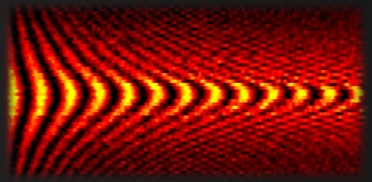

operation	current fidelity	reference
Single-qubit gates	99.93%	Yoneda et al. Nat. Nanotechnol. **13** (2018).
Two-qubit gates CROT	**98.0% (RBM)**	Huang et al., Nature ***569*** (2019).
Two-qubit gate SWAP	**< 90%**	Sigillito et al., npj Quant. Inform. **5** (2019).
Elzerman **readout**	**< 90%**	Keith et al., New J. of Phys. **21** (2019).
QND **readout**	**>95%**	Nakajima et al., Nat. Nano. **14** (2019).
Initialization	**<99% (at 55ms)**	Keith et al., New J. of Phys. **21** (2019).

Fault-tolerant qubits:

- F_S (1-qubit) > 99%, (99.9%?)
- F_{2Q} *(2-qubit) > 99%*
- F_{init} *(Initialization) > 99%*
- F_{RO} *(read-out) > 99%*

Fowler *et al.*, Phys. Rev. A **87** (2009).

Two-qubit gate fidelity (UNSW device)

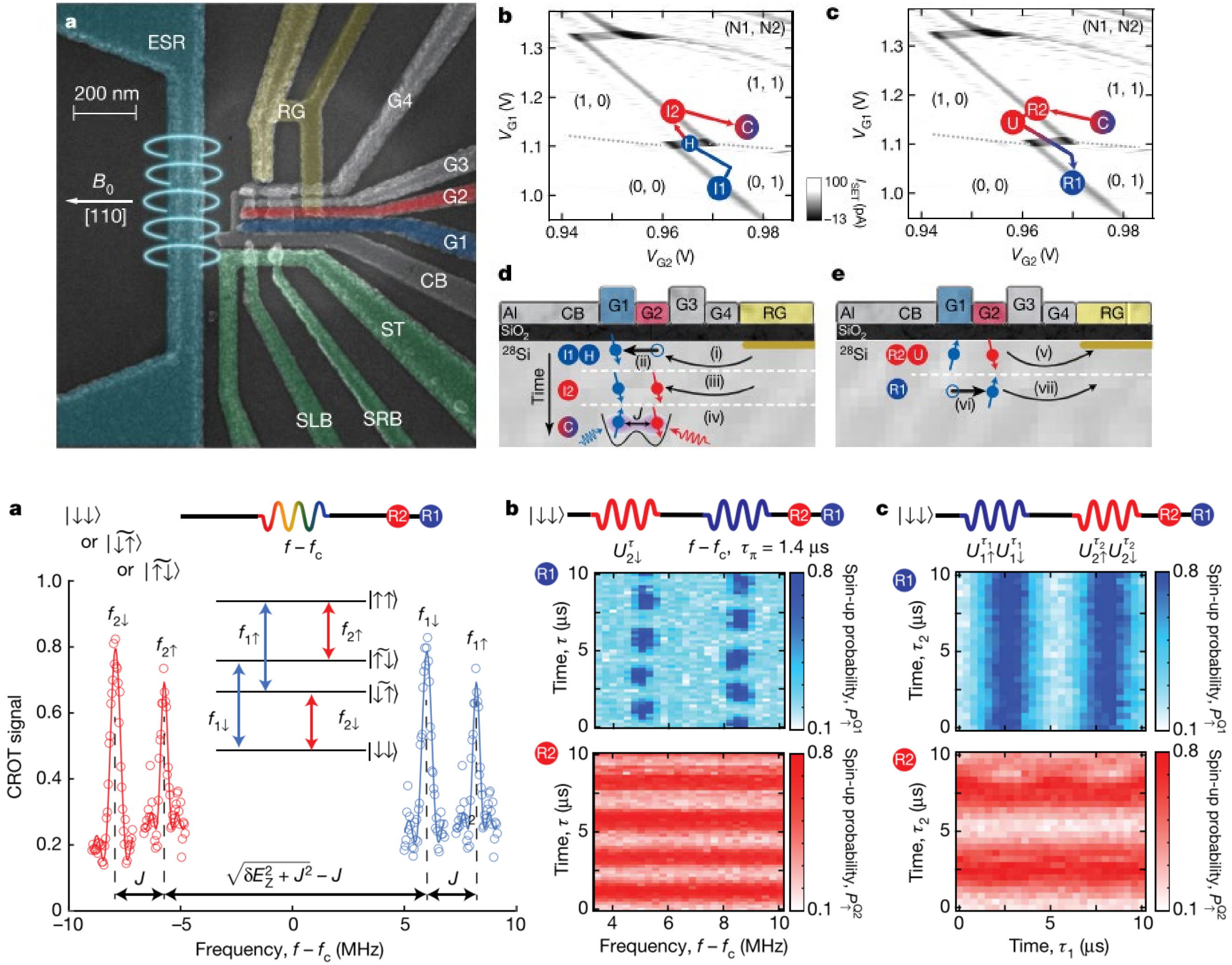

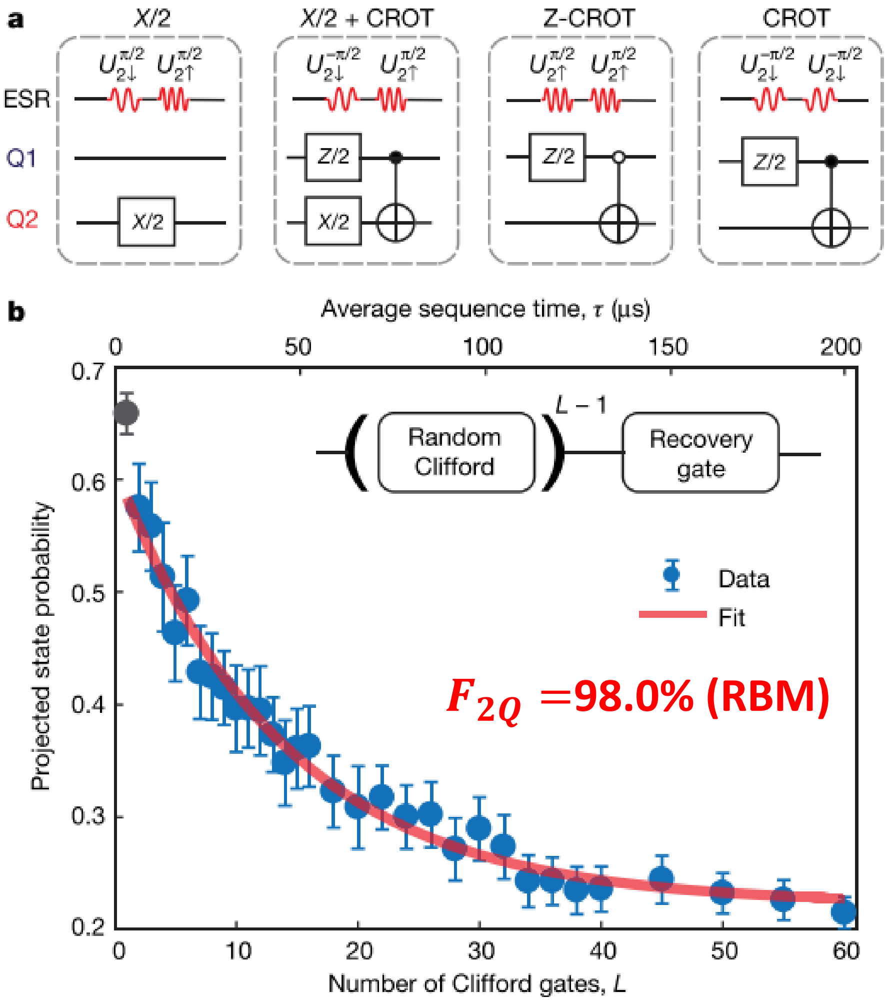

UNSW: Huang et al., Fidelity benchmarks for two-qubit gates in silicon. *Nature*, ***569*** (2019)

CNOT~1MHz

Loss–DiVincenzo Qubits – an overview

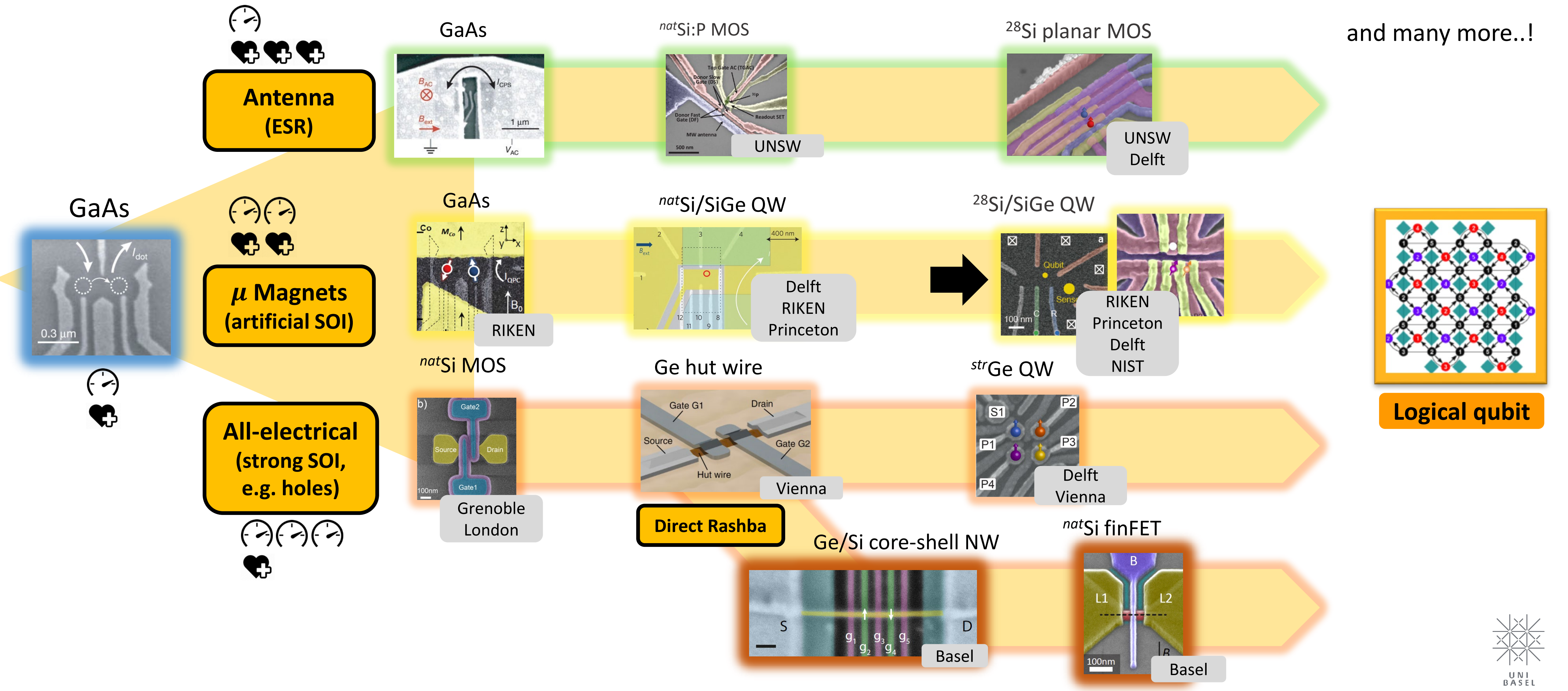

SOI: spin-orbit interaction NW: nanowire QW: quantum well

Device

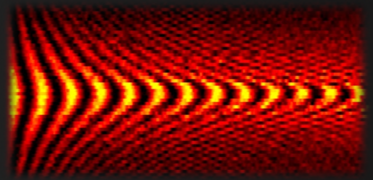

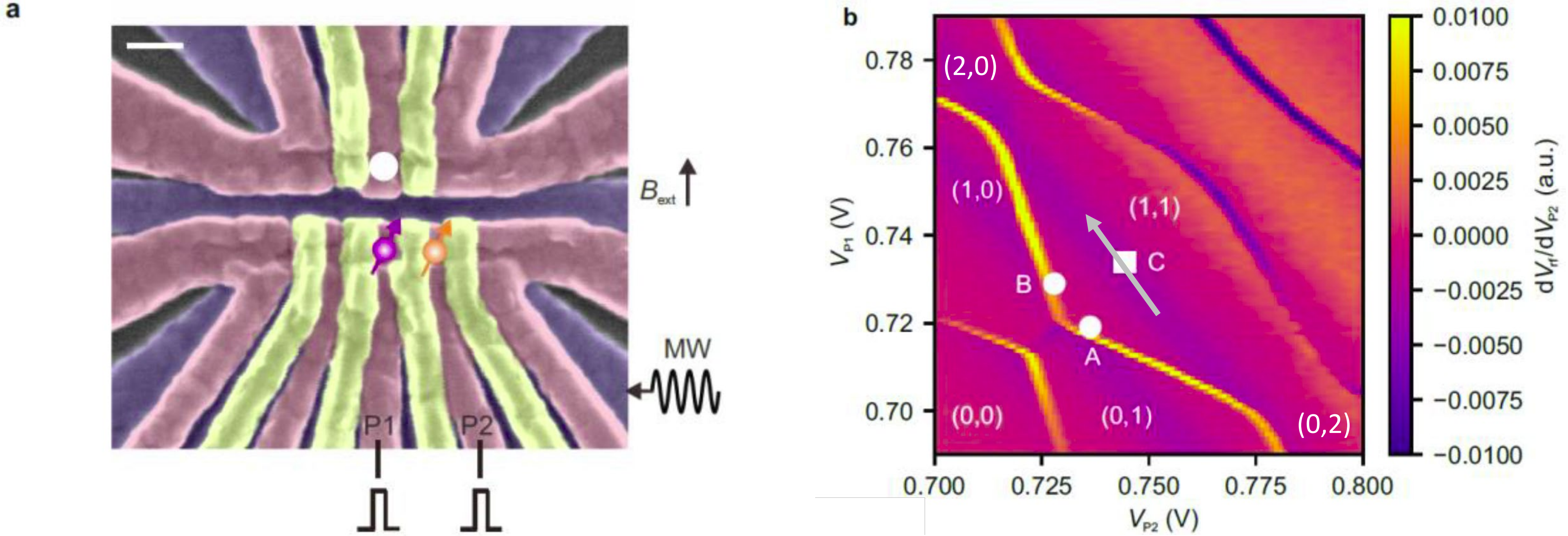

Silicon-28 QW (800 ppm)
Overlapping Al gates (3 layers, native Al_2O_3)
Cobalt-Micromagnet (not shown)

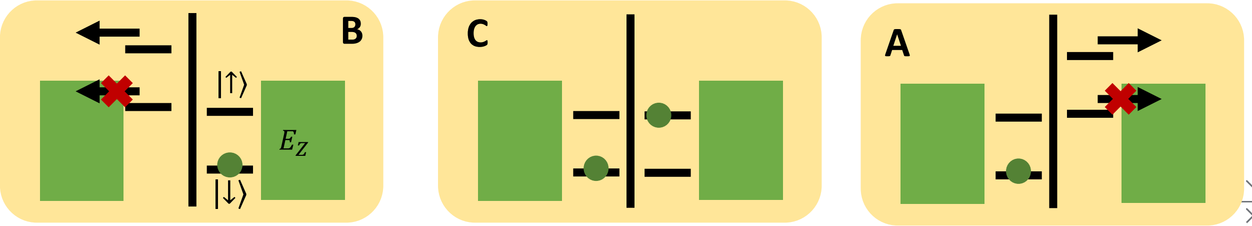

CROT

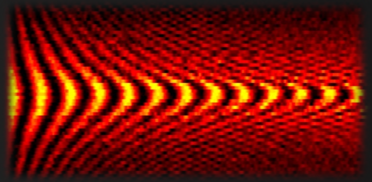

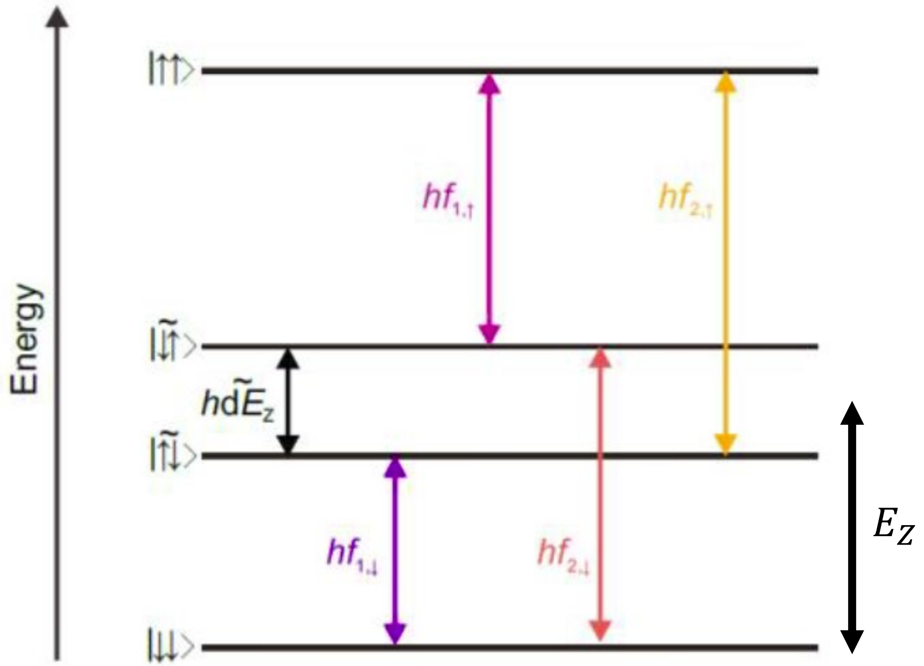

$$f_{m,\sigma} = E_Z \pm \left(d\tilde{E}_Z \pm J\right)/2$$

m = addressed qubit
σ = control spin

effective Zeeman difference: $d\tilde{E}_Z = \sqrt{dE_Z^2 + J^2}$

J: exchange
dE_Z: Zeeman-difference (micromagnet)

Example: $f_{1,\downarrow}$ drives qubit 1 if qubit 2 is $|\downarrow\rangle$ (CROT)

CROT gates

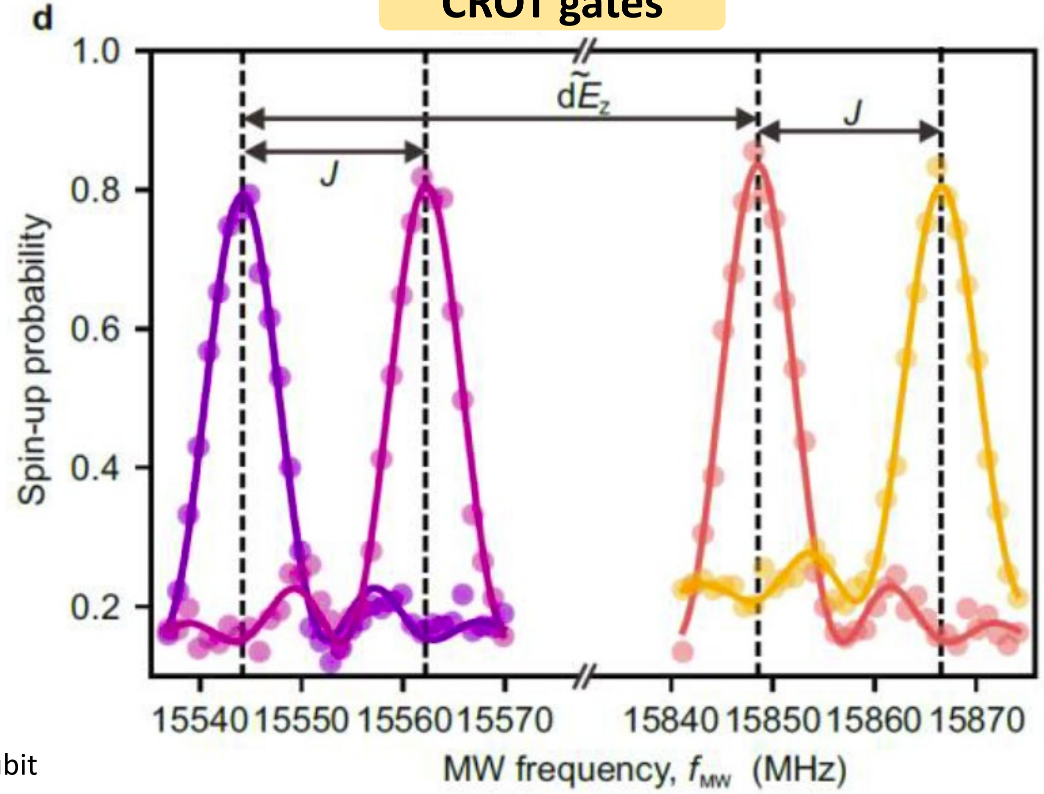

$E_Z \approx 15.7$ GHz
$d\tilde{E}_Z \approx 300$ MHz
$J \approx 1$ MHz..30 MHz

UNI BASEL

CROT: unwanted rotation of target qubit

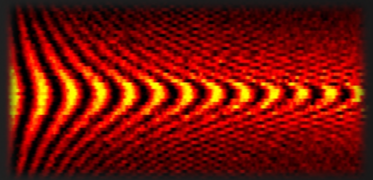

EDSR-control: time dependent rotating frame

$$R = \text{diag}\ \left(e^{-i2\pi E_Z t}, e^{-i\pi(-d\ddot{E}_Z - J)t}, e^{-i\pi(d\ddot{E}_Z - J)t}, e^{i2\pi E_Z t}\right)$$

Time dependent Hamiltonian

$$H_R(t) = RHR^\dagger - \frac{ih}{2\pi}\frac{\partial R}{\partial t}R^\dagger$$

$$= \frac{h}{2}\begin{pmatrix} 0 & f_R e^{-i2\pi(f_{2,\uparrow}-f_{MW})t+i\phi} & f_R e^{-i2\pi(f_{1,\uparrow}-f_{MW})t+i\phi} & 0 \\ f_R e^{i2\pi(f_{2,\uparrow}-f_{MW})t-i\phi} & 0 & 0 & f_R e^{-i2\pi(f_{1,\downarrow}-f_{MW})t+i\phi} \\ f_R e^{i2\pi(f_{1,\uparrow}-f_{MW})t-i\phi} & 0 & 0 & f_R e^{-i2\pi(f_{2,\downarrow}-f_{MW})t+i\phi} \\ 0 & f_R e^{i2\pi(f_{1,\downarrow}-f_{MW})t-i\phi} & f_R e^{i2\pi(f_{2,\downarrow}-f_{MW})t-i\phi} & 0 \end{pmatrix}.$$

Off-diagonal terms → CROT

For $f_R \approx J$: J term leads to (unwanted) off-resonant rotations.

Tilted axis with effective $\tilde{f}_R = \sqrt{f_R^2 + J^2}$

CROT $\pi/2$ time: $t_{hp} = 1/(4f_R)$

$\tilde{f}_R \cdot t_{hp} = n, \quad n \in \mathbb{N}$

$f_R = J/\sqrt{16n^2 - 1}$

Therefore

$f_R = J/\sqrt{15}$ fixed

See also Huang et al., Fidelity benchmarks for two-qubit gates in silicon. *Nature*, ***569*** (2019)

“Single-Qubit” and two-qubit gates

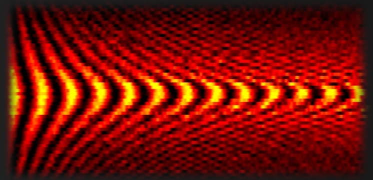

Spin relaxation

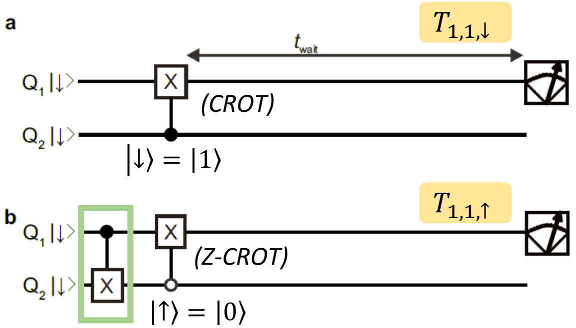

$T_1 > 10\ ms$

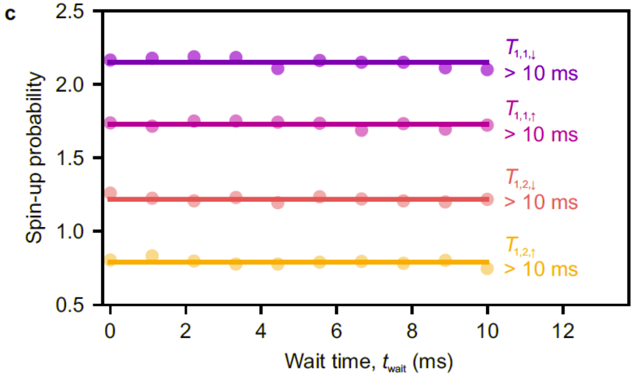

Free induction decay

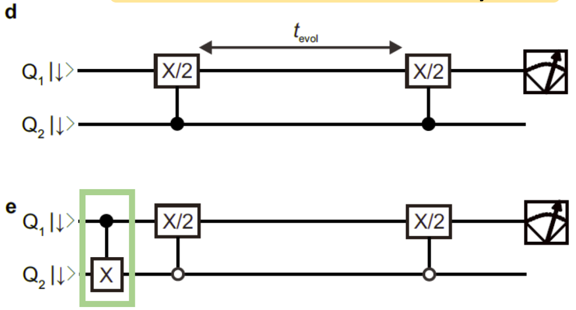

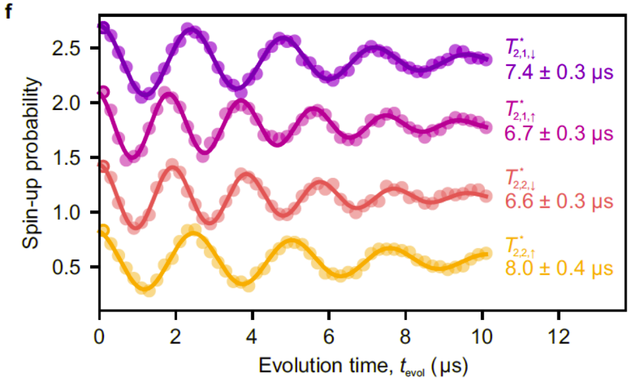

$T_2^* \approx 6.5-8\ \mu s$

Hahn-echo

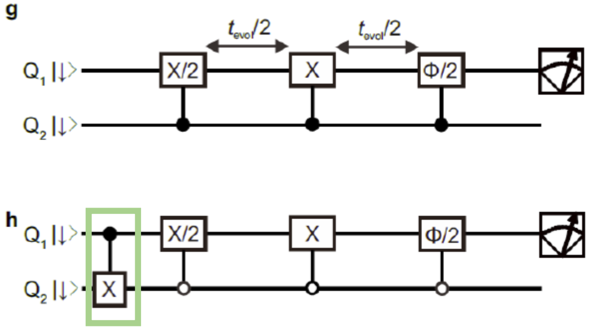

$T_2^{Hahn} \approx 30\ \mu s$

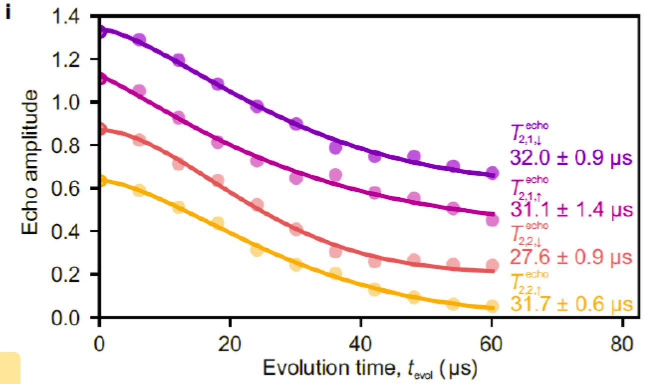

Rabi-decay

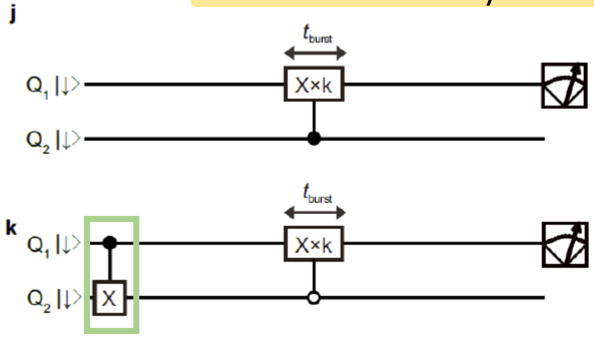

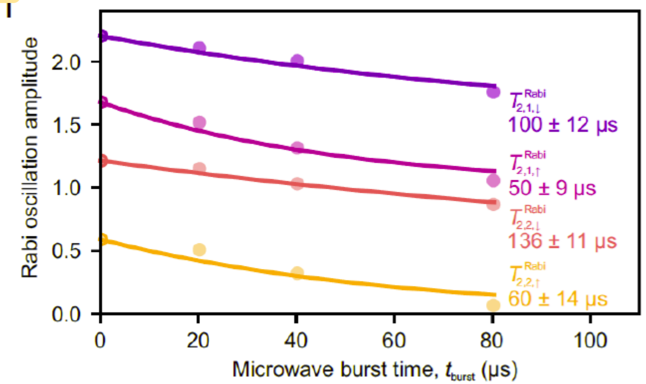

$T_2^{Rabi} \approx 50-130\ \mu s$

J=18.85 MHz, f_R=4.867 MHz

For f_R = 5 MHz → $Q_X \approx$ 99.8 ... 99.92%

UNI BASEL

Exchange coupling J

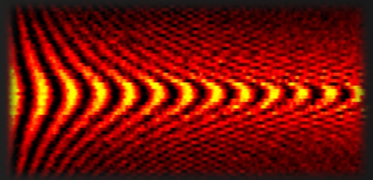

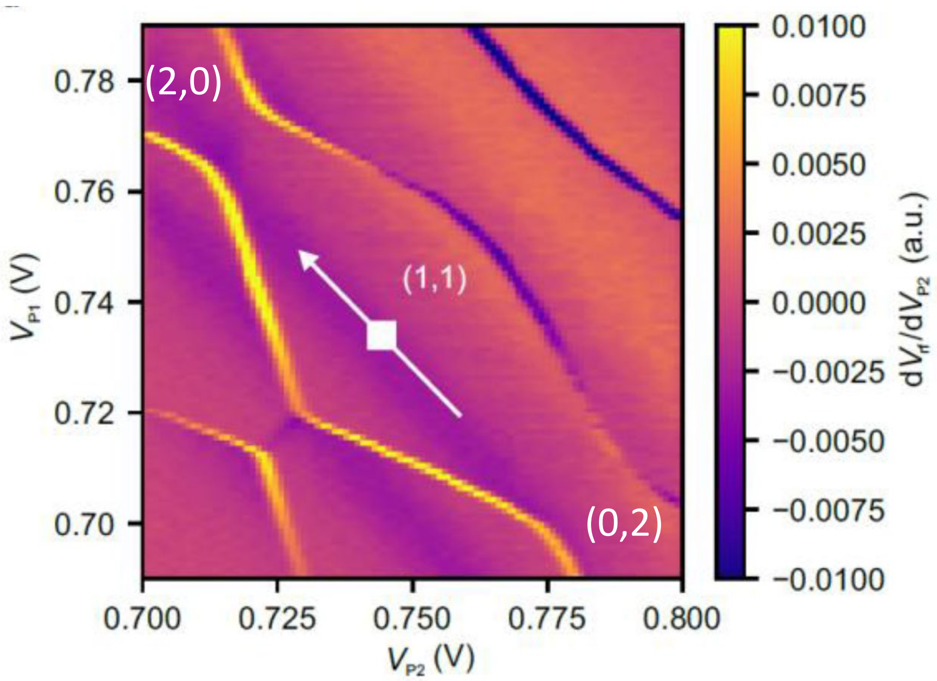

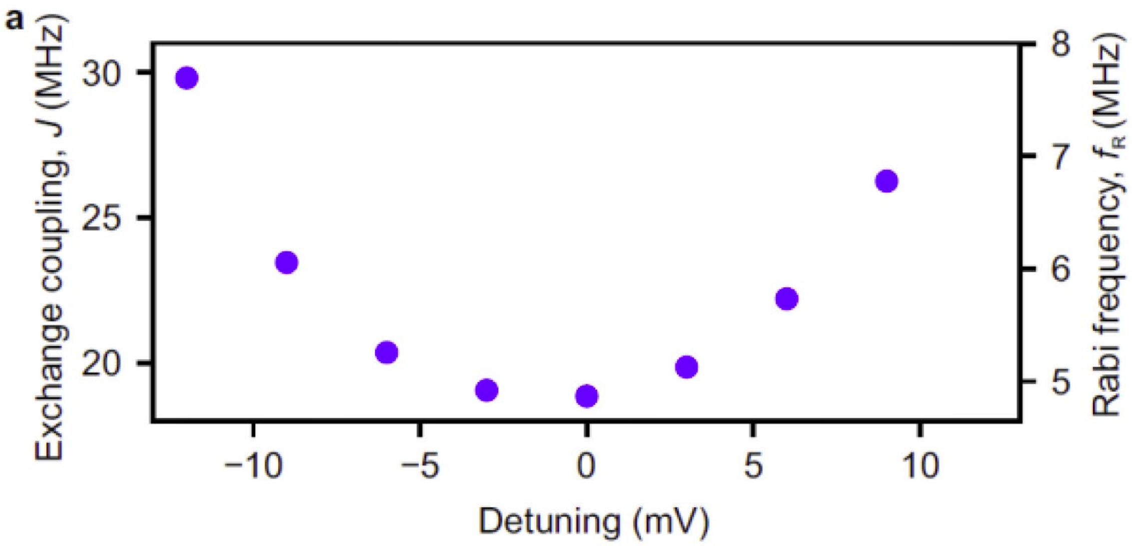

$f_R = J/\sqrt{15}$ **fixed**

Detuning dependence of the coherence

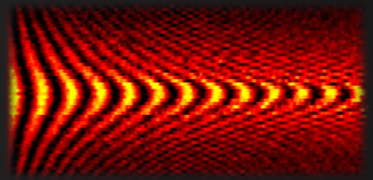

EDSR spectra – detuning dependence

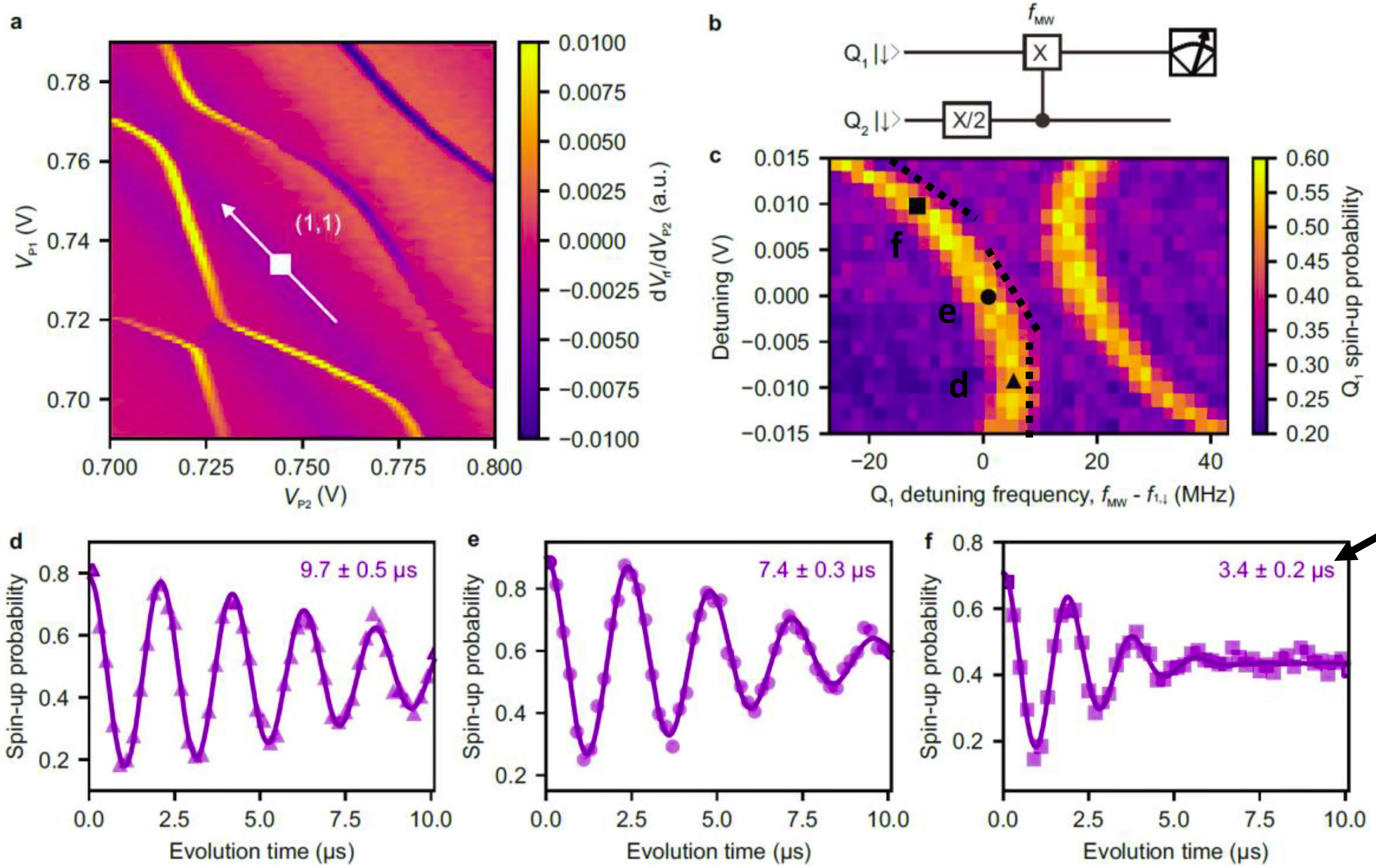

$$f_{m,\sigma} = E_Z \pm (d\tilde{E}_Z \pm J)/2$$

$$d\tilde{E}_Z = \sqrt{dE_Z^2 + J^2}$$

$T^*_{2,1,\downarrow}$

Ramsey fringes

T_2^* limited by detuning charge noise

Dephasing and Rabi decay

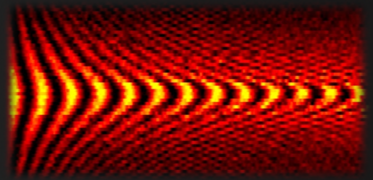

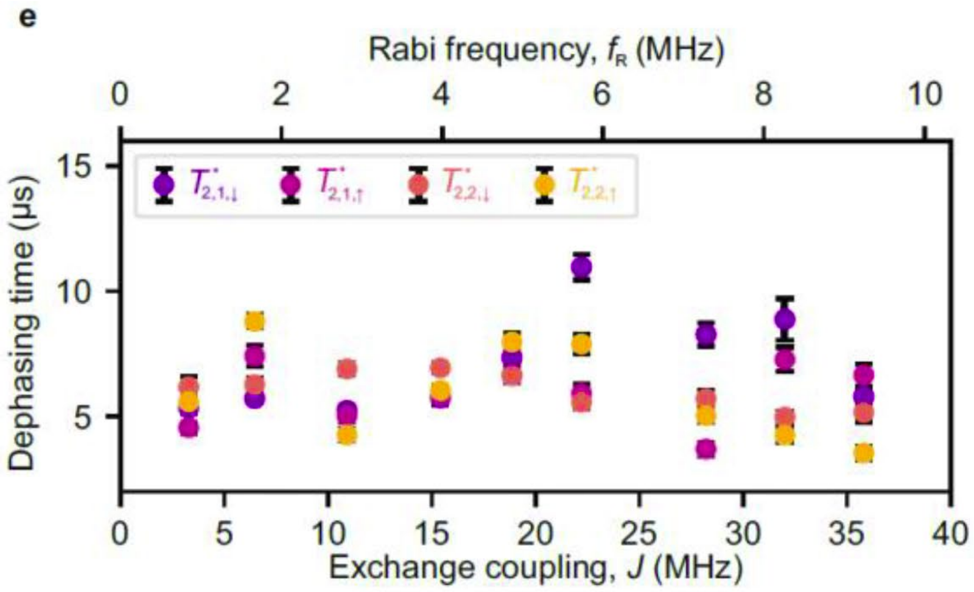

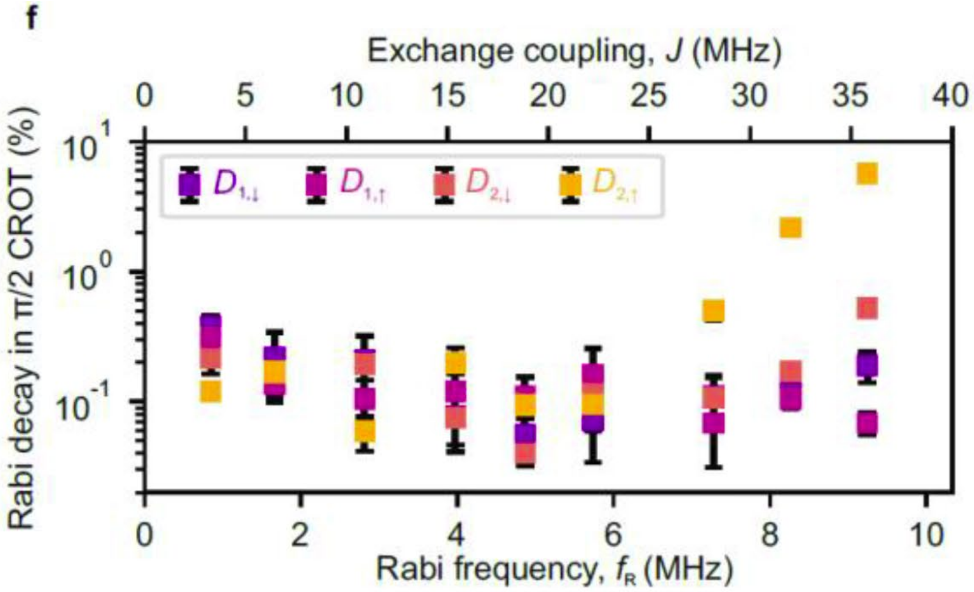

Dephasing independent of exchange J

Limiting: fluctuations in f_m not J
$\Delta f_{m,\sigma} = \Delta f_m \pm \Delta J/2$

CROT too slow

optimal

Rabi too fast

Rabi decay depends on Rabi frequency

Fault-tolerant threshold?

Single qubit gates (unconditional)

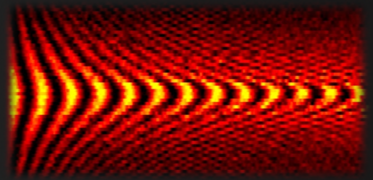

Unconditional $X/2$

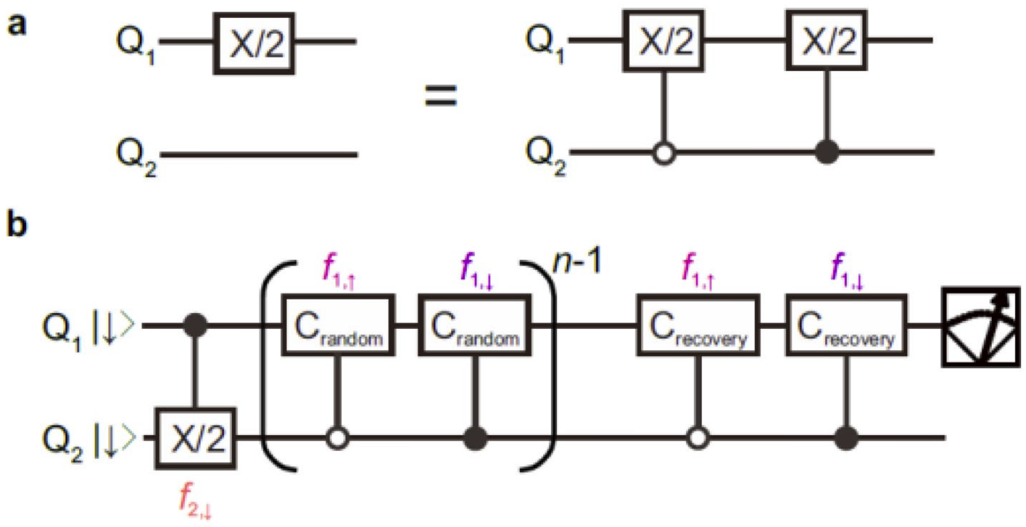

Fast frequency switch by **sideband modulation** (-230 MHz to 180 MHz)

(1.875 primitive gates per Clifford)

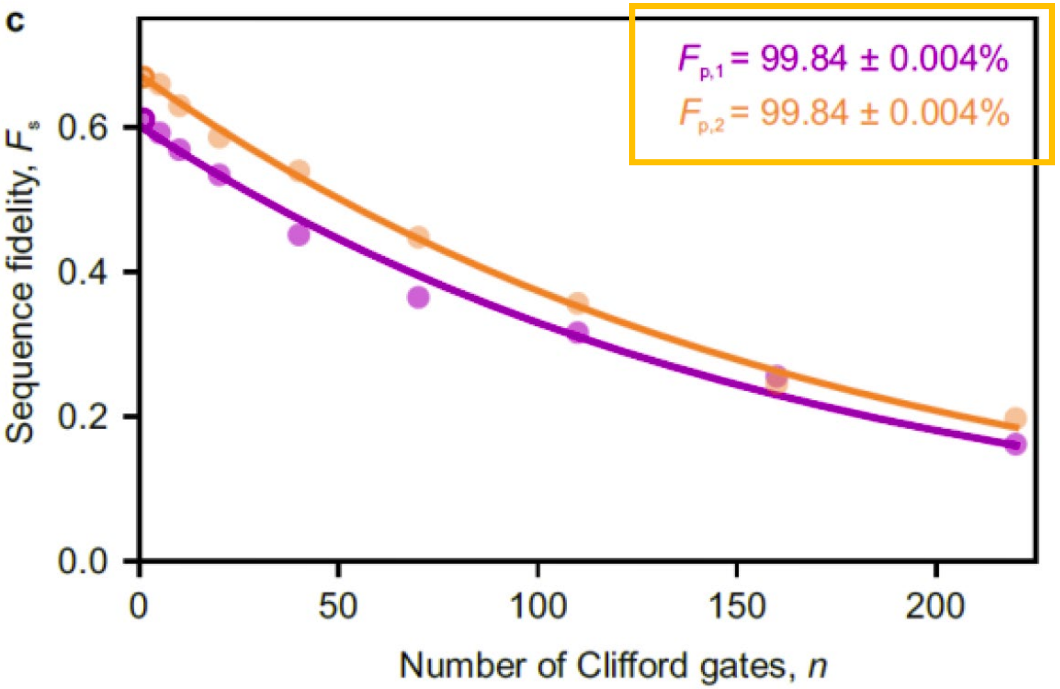

Unconditional fidelity $F = 99.84\%$

Single-tone single-qubit gate performance

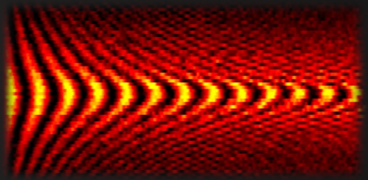

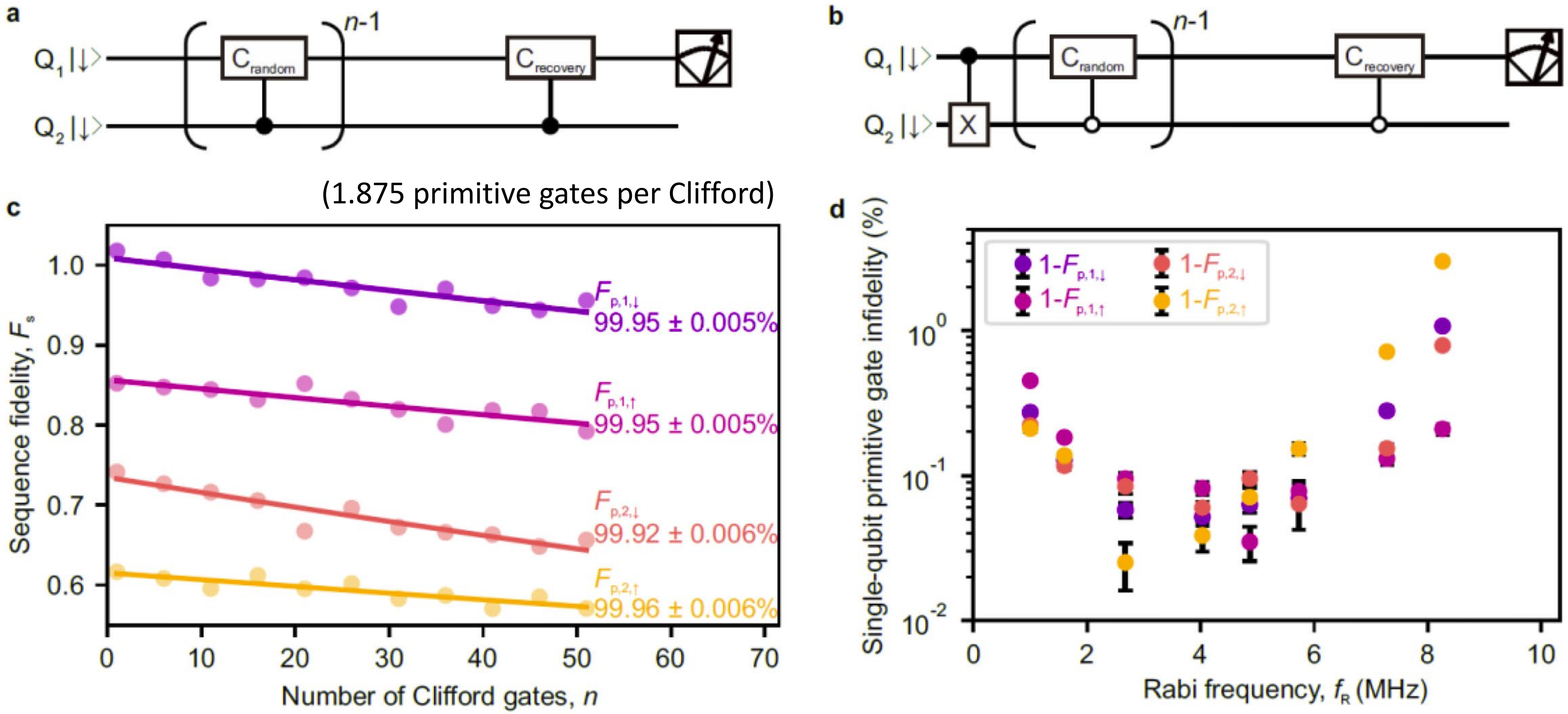

(1.875 primitive gates per Clifford)

Fidelity of “**conditional**” Gates $\mathrm{F} \approx 99.94\% > 99.9\%$

Remember: unconditional fidelity $F = 99.84$

Two-qubit primitive gates and RBM

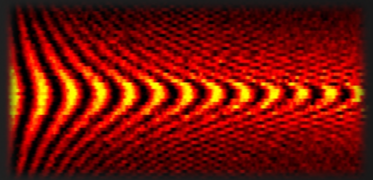

two-qubit primitives

two-qubit RBM

interleaved two-qubit RBM

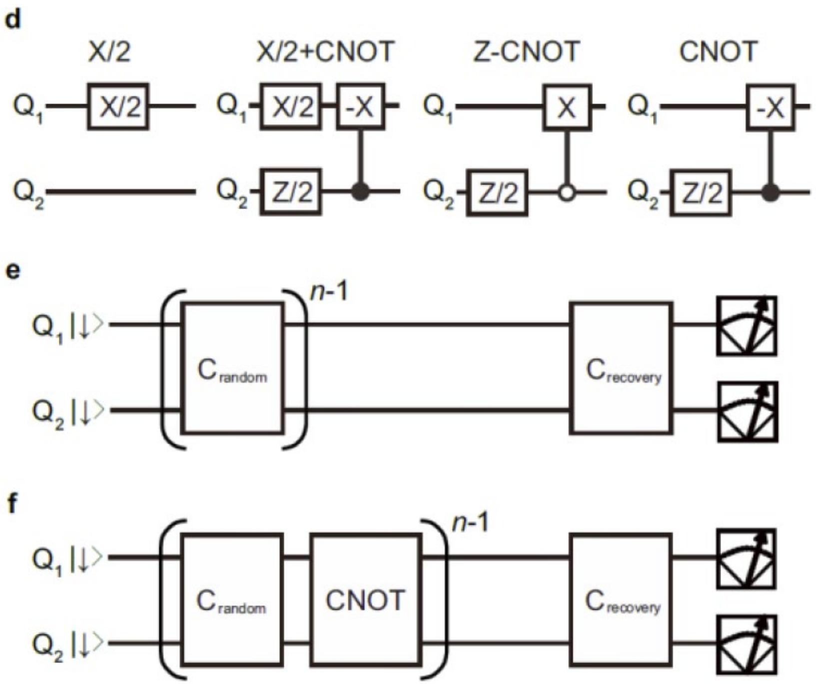

(2.57 primitive gates per Clifford)

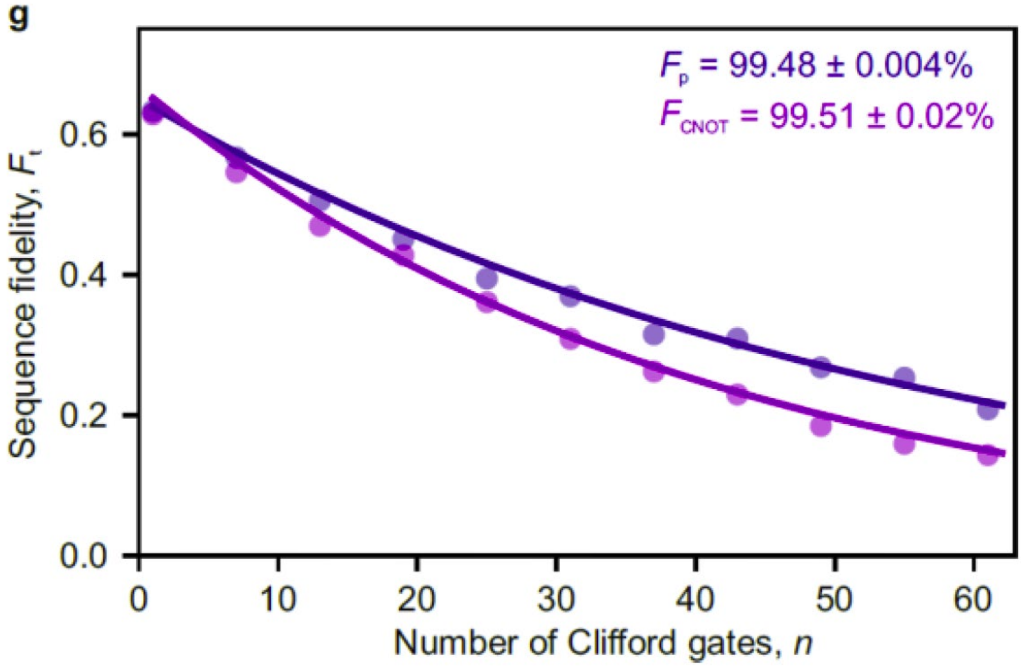

Two-qubit gate fidelity $F = 99.5\%$

Fidelity dependence on Rabi frequency and exchange coupling

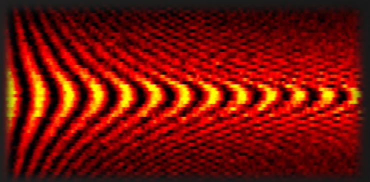

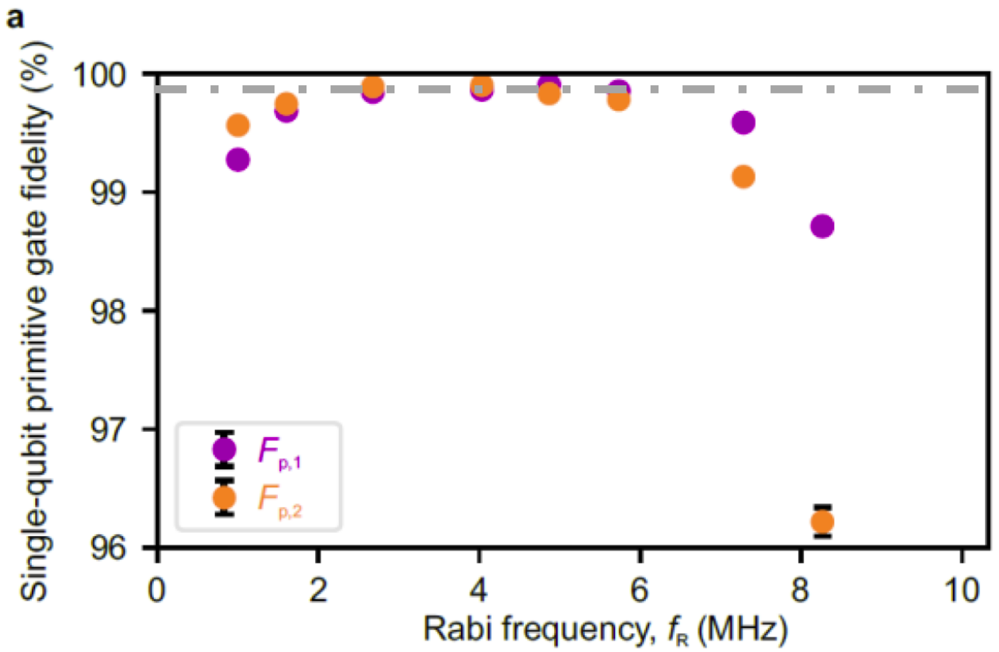

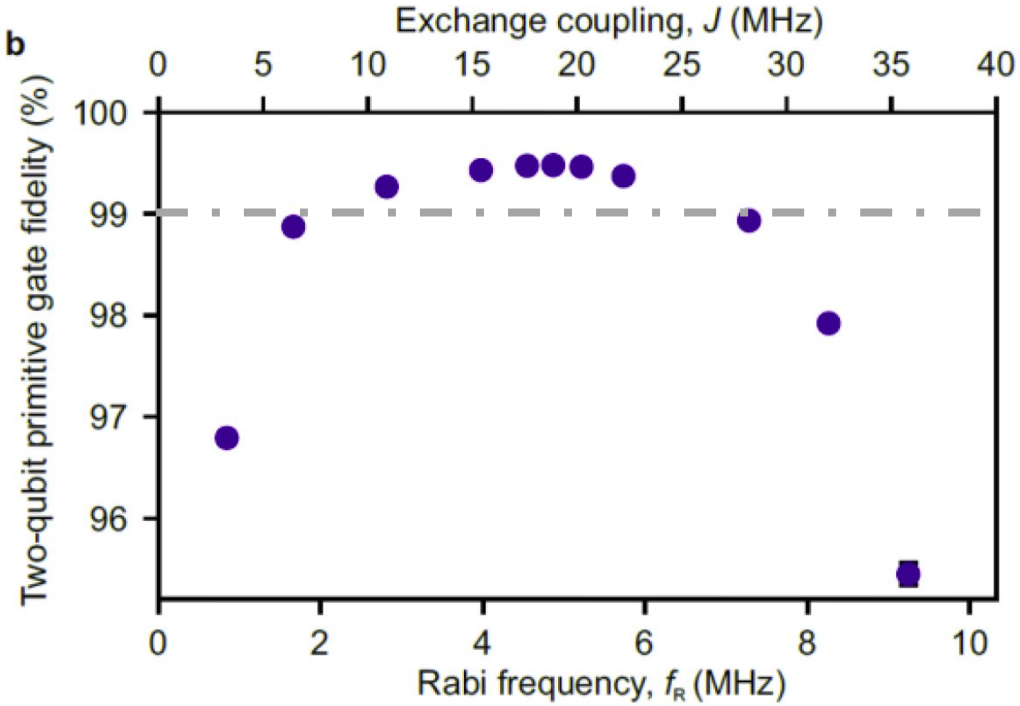

Single-tone single-qubit primitive gate fidelities

$$F_{p,m} = F_{p,m,\downarrow} \cdot F_{p,m,\uparrow}$$

For $f_R = 2.8 - 5.7$ MHz:

exceeding fault tolerant threshold

Two-qubit quantum processor

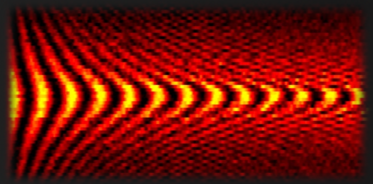

Feb **2018**, 305 citations (Sept. 2021)

LETTER

doi:10.1038/nature25766

A programmable two-qubit quantum processor in silicon

T. F. Watson[1], S. G. J. Philips[1], E. Kawakami[1], D. R. Ward[2], P. Scarlino[1], M. Veldhorst[1], D. E. Savage[2], M. G. Lagally[2], Mark Friesen[2], S. N. Coppersmith[2], M. A. Eriksson[2] & L. M. K. Vandersypen[1]

Now that it is possible to achieve measurement and control fidelities for individual quantum bits (qubits) above the threshold for fault tolerance, attention is moving towards the difficult task of scaling up the number of physical qubits to the large numbers that are needed for fault-tolerant quantum computing. In this context, quantum-dot-based spin qubits could have substantial advantages over other types of qubit owing to their potential for all-electrical operation and ability to be integrated at high density onto an industrial platform. Initialization, readout and single and two-qubit gates have been demonstrated in various quantum dot- based qubit representations. However, as seen with small-scale demonstrations of quantum computers using other types of qubit, combining these elements leads to challenges related to qubit crosstalk, state leakage, calibration and control hardware. Here we overcome these challenges by using carefully designed control techniques to demonstrate a programmable two-qubit quantum processor in a silicon device that can perform the Deutsch–Josza algorithm and the Grover search algorithm—canonical examples of quantum algorithms that outperform their classical analogues. We characterize the entanglement in our processor by using quantum state tomography of Bell states, measuring state fidelities of 85–89% and concurrences of 73–82%.

These results pave the way for larger-scale quantum computers that use spins confined to quantum dots.

Deutsch-Josza

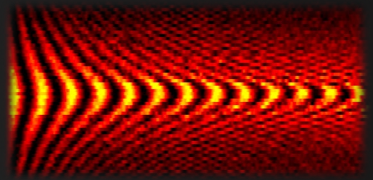

Two sides of a coin: same or different?
Classical: look at both sides → 2 measurements
Quantum: create superposition → 1 measurement

Mathematically: function constant or balanced?

→ Is $f(0) = f(1)$?

$\boldsymbol{f_2}$

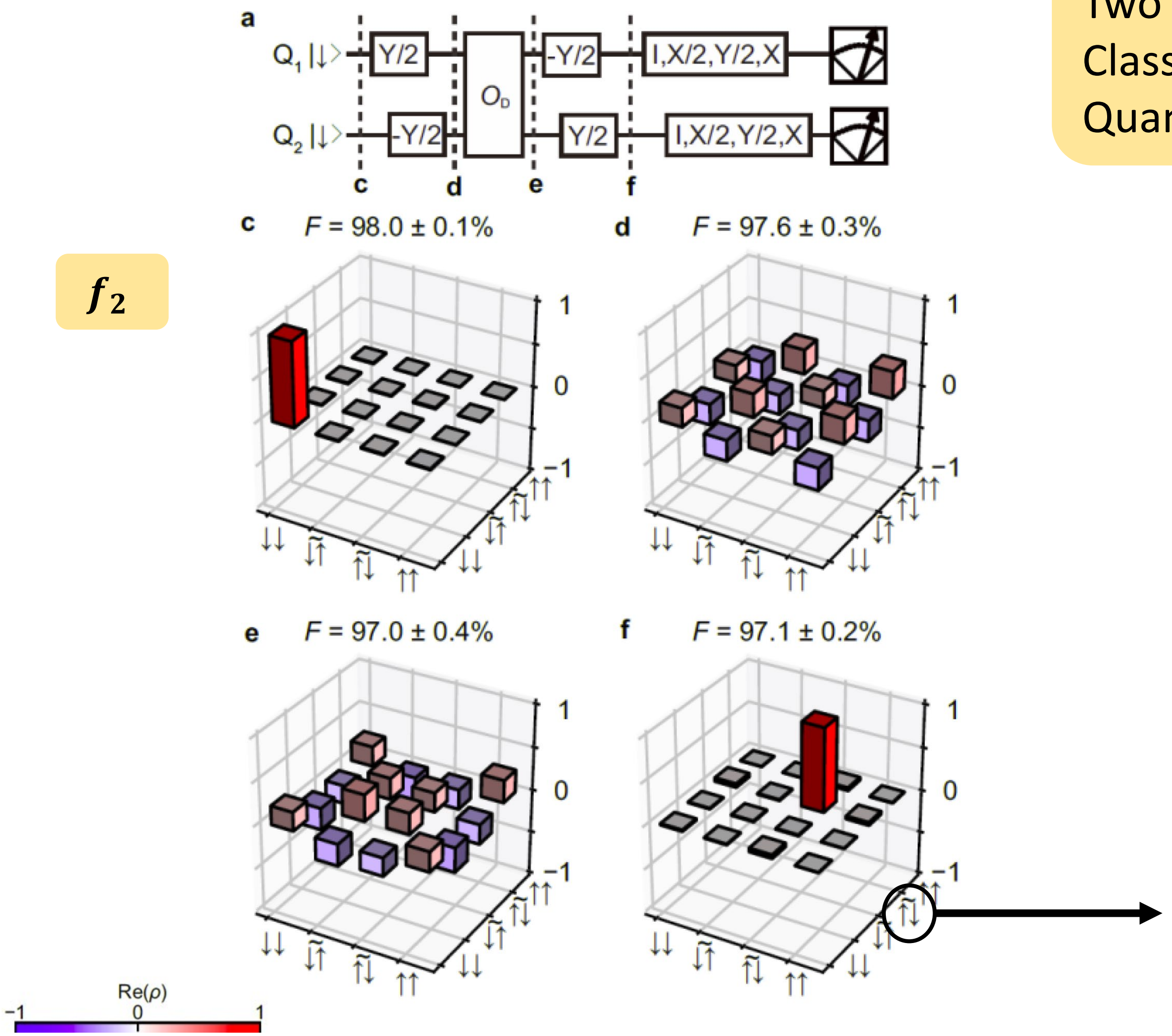

Constant function	Implementation $\boldsymbol{O_D}$
$f_0(x) = 1$	I_2
$f_1(x) = 0$	X_2
Balanced function	
$f_2(x) = x$	$Z - CNOT_2$
$f_3(x) = 1 - x$	$CNOT_2$

$x \in \{0,1\} = \{|\uparrow\rangle, |\downarrow\rangle\}$

Result

$Q_1|\downarrow\rangle = |1\rangle$ = constant function

$\boldsymbol{Q_1|\uparrow\rangle = |0\rangle}$ **= balanced function**

$CNOT_2$ = target Q2

UNI BASEL

Deutsch-Jozsa

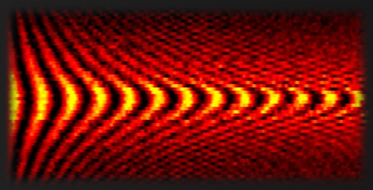

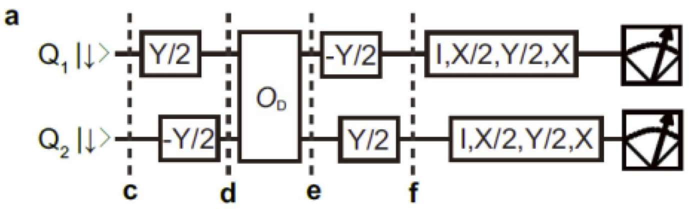

f_0

f_1

Q1 in |↓⟩

f_2

f_3

Q1 in |↑⟩

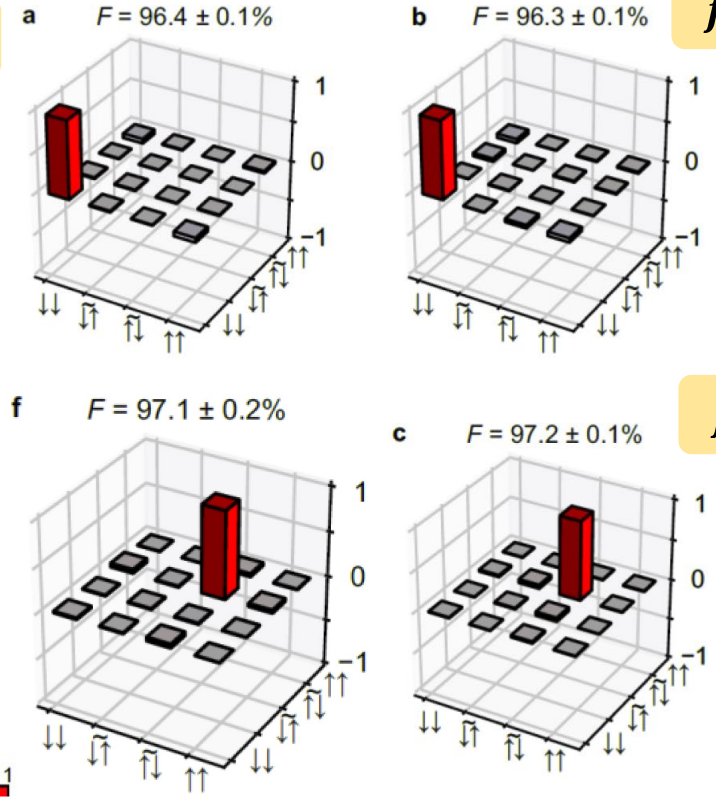

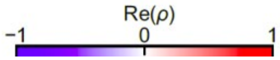

Two sides of a coin: same or different?
Classical: look at both sides → 2 measurements
Quantum: create superposition → 1 measurement

Mathematically: function constant or balanced?

→ Is $f(0) = f(1)$?

Constant function	**Implementation O_D**
$f_0(x) = 1$	I_2
$f_1(x) = 0$	X_2
Balanced function	
$f_2(x) = x$	$Z - CNOT_2$
$f_3(x) = 1 - x$	$CNOT_2$

$x \in \{0,1\} = \{|\uparrow\rangle, |\downarrow\rangle\}$

Result

$Q_1|\downarrow\rangle = |1\rangle$ = constant function
$Q_1|\uparrow\rangle = |0\rangle$ = balanced function

$CNOT_2 =$ target Q2

UNI BASEL

Deutsch-Jozsa

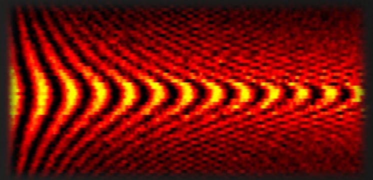

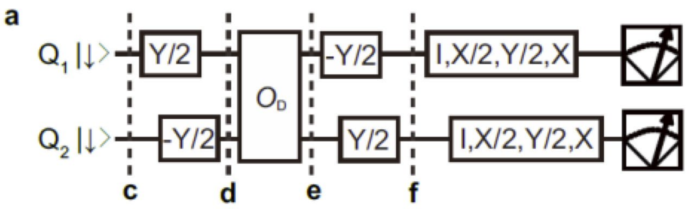

f_0

Q1 in |↓⟩

f_1

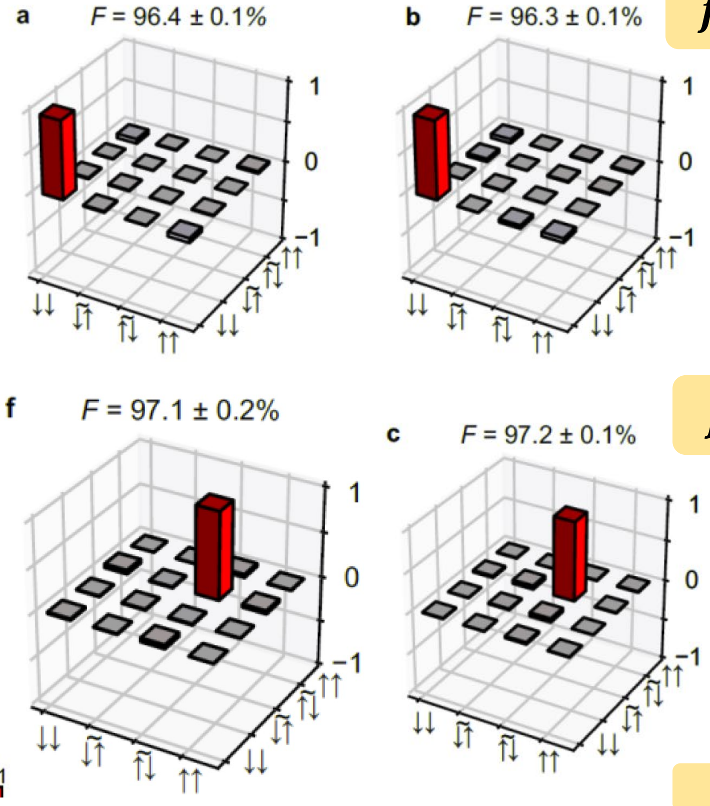

f_2

Q1 in |↑⟩

f_3

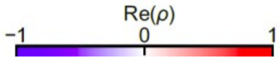

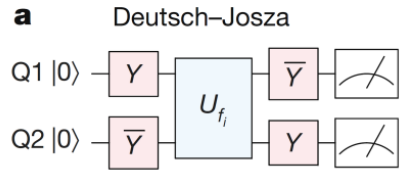

Watson *et al.*, Nature (2018)

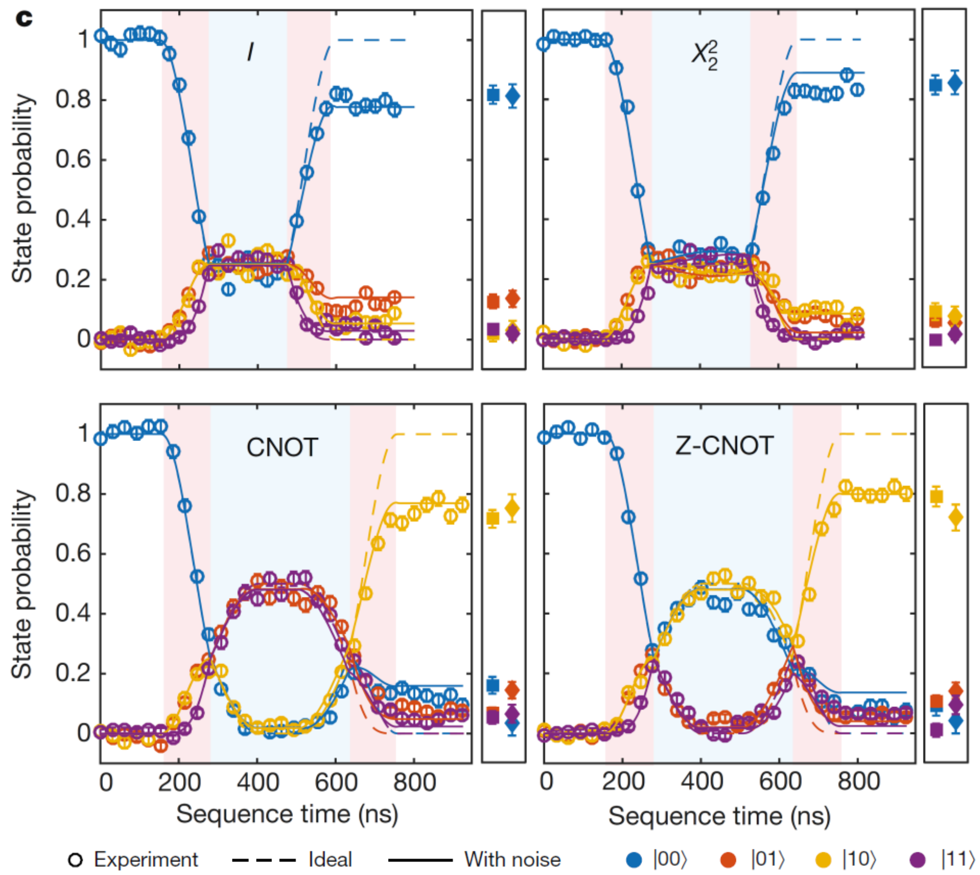

Much higher state-fidelity than previously !

Grover search algorithm – small theory

Oracle function
$f(x \neq x_0) = 0$
$f(w) = 1$

"Database"							
Input value x	1	2	…	$\boldsymbol{x_0}$	…	$N-1$	N
$f(x)$	0	0	0	**1**	0	0	0

Classical: $O(N)$
Quantum: $O(\sqrt{N})$
1M operations → 1k operations

2-Qubit Grover

e.g. O_{00}

Input	Output
$\|00\rangle$	1
$\|01\rangle$	0
$\|10\rangle$	0
$\|11\rangle$	0

Grover search algorithm

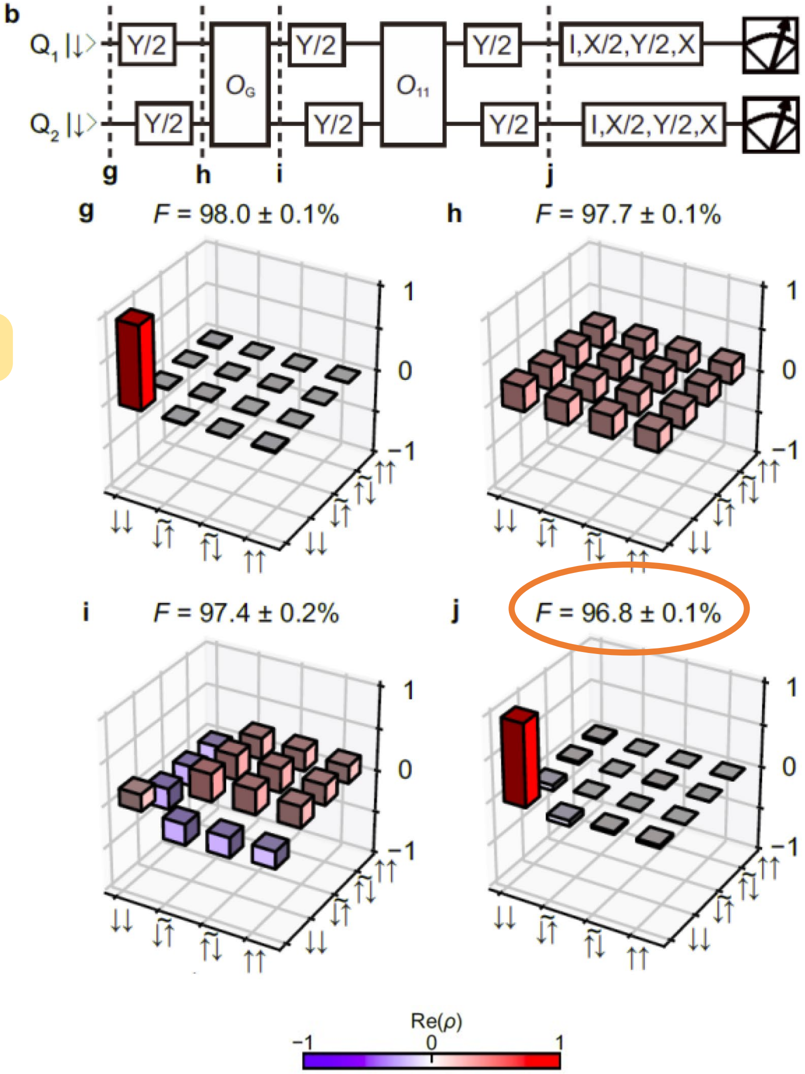

f_{11}

Find unique input value x_0 of a function $f(x)$ such that $f(x_0) = 1$ and $f(x \neq x_0) = 0$ otherwise.

Here: Algorithm returns marked state: $f_{11} \rightarrow |11\rangle = |\downarrow\downarrow\rangle$

Oracle functions

$$O_{11} = (Y_2/2)(CNOT_2)(-Y_2/2)$$
$$O_{10} = (Y_1/2)(Z - CNOT_1)(-Y_1/2)$$
$$O_{01} = (-Y_1/2)(CNOT_1)(-Y_1/2)$$
$$O_{00} = (-Y_2/2)(Z - CNOT_2)(-Y_2/2)$$

$$x = ij \ \ (i, j \in \{0,1\})$$

Grover search algorithm

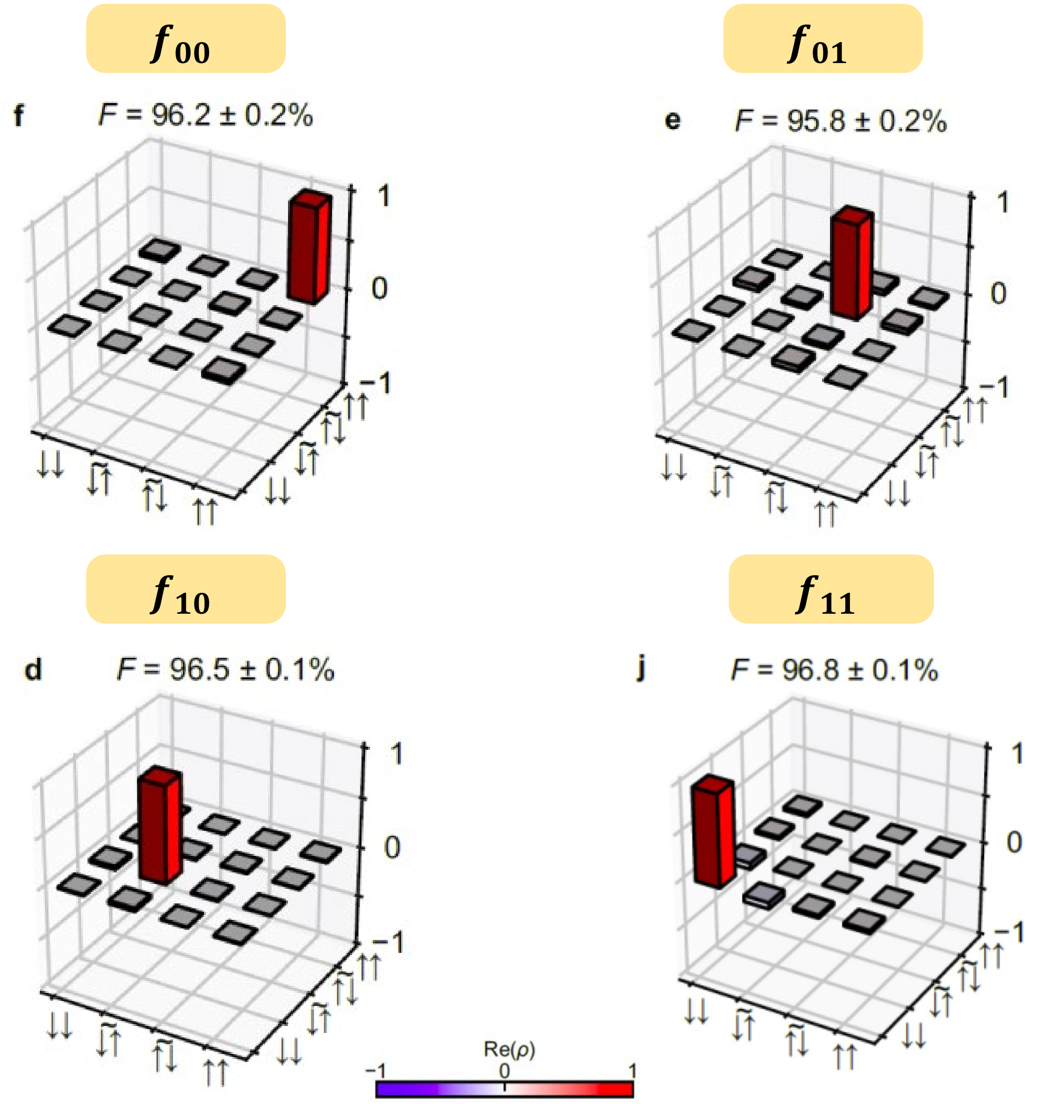

Watson *et al.*, Nature (2018)

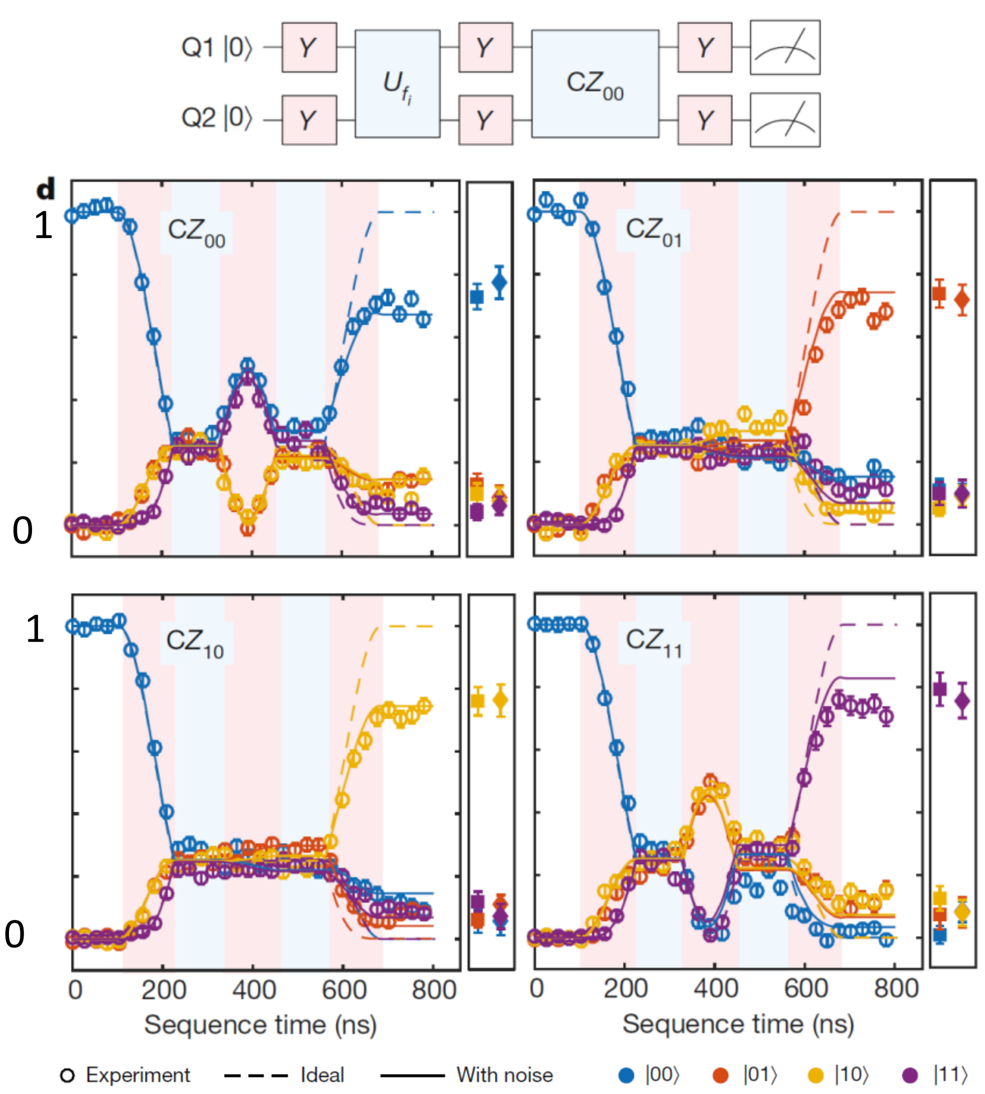

Summary

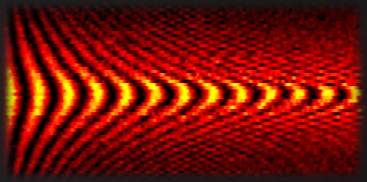

- Two-qubit gate fidelity limited by single-qubit fidelity (Δf)
- Reaching «Surface code error correction threshold»
  - First time two-qubit gate fidelity F_{2Q} > 99%
  - Single-gate fidelity F_{1Q} > 99.9%
- Implementation of high fidelitiy two-qubit quantum algorithms
- Future: high-F CNOT with pulsed exchange control

Appendix

Basis states: $|\uparrow\uparrow\rangle, |\uparrow\downarrow\rangle, |\downarrow\uparrow\rangle, |\downarrow\downarrow\rangle$

$$H = \frac{h}{2}\begin{pmatrix} 2E_z & \Omega & \Omega & 0 \\ \Omega^* & -d\tilde{E}_Z - J & 0 & \Omega \\ \Omega^* & 0 & d\tilde{E}_Z - J & \Omega \\ 0 & \Omega^* & \Omega^* & -2E_Z \end{pmatrix}$$

$$hd\tilde{E}_Z = h\sqrt{dE_Z^2 + J^2}$$

$$\Omega = f_R\, e^{i2\pi f_{MW}t + i\phi}$$ (MW drive)

Deutsch-Jozsa

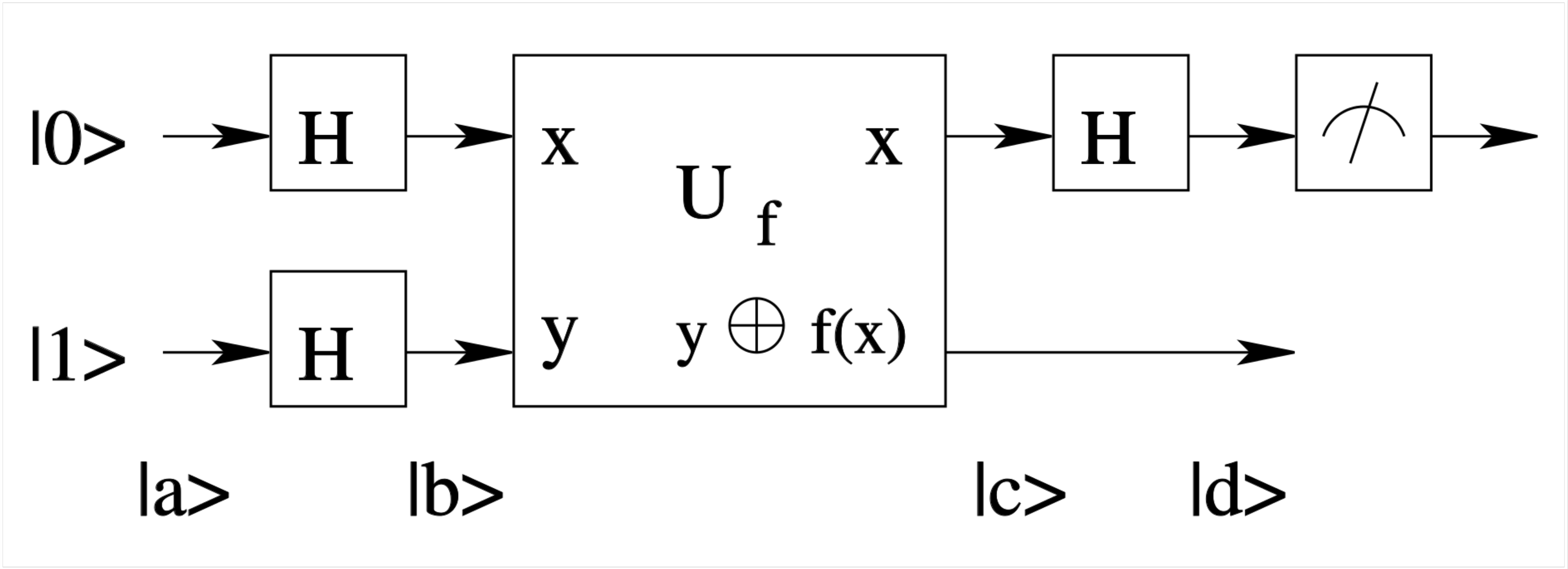

Deutsch-Josza

Two sides of a coin: same or different?
Classical: look at both sides → 2 measurements
Quantum: create superposition → 1 measurement

Mathematically: function constant or balanced?

Constant function	**Qubit gate**
$f_1(0) = f_1(1) = 0$	I
$f_2(0) = f_2(1) = 0$	X_2^2
Balanced function	
$f_3(0) = 0, f_3(1) = 1$	$CNOT = Y_2 CZ_{11} \overline{Y}_2$
$f_4(0) = 1, f_4(1) = 0$	$ZCNOT = \overline{Y}_2 CZ_{00} Y_2$

Q2 Target for CNOT and Z-CNOT
Input Qubit (Q1) after gate:
$|0\rangle$ = constant function
$|1\rangle$ = balanced function

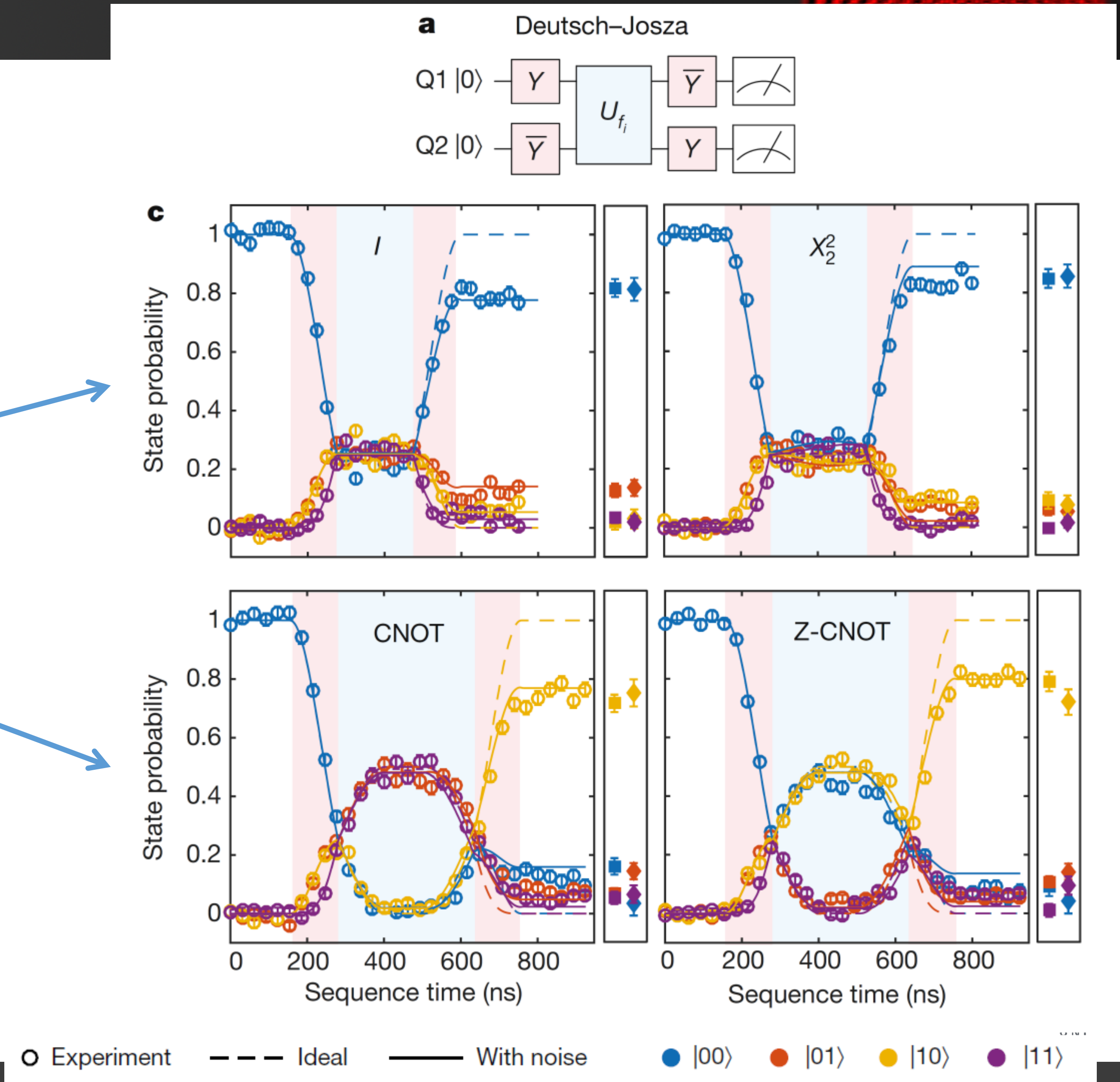

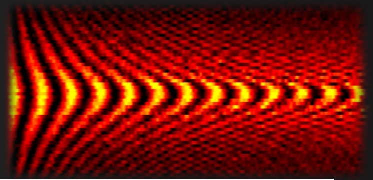

- Find unique input value x_0 of a function $f(x)$ that gives $f(x_0) = 1$ and $f(x \neq x_0) = 0$ otherwise
- Four output states $x \in \{00,01,10,11\}$
  → four functions f_{ij}
- $CZ_{ij}|x\rangle = (-1)^{f_{ij}(x)}|x\rangle$
  - → negative phase for $f_{ij}(x) = 1$
- The sequence returns the state $|ij\rangle$ when applying CZ_{ij}

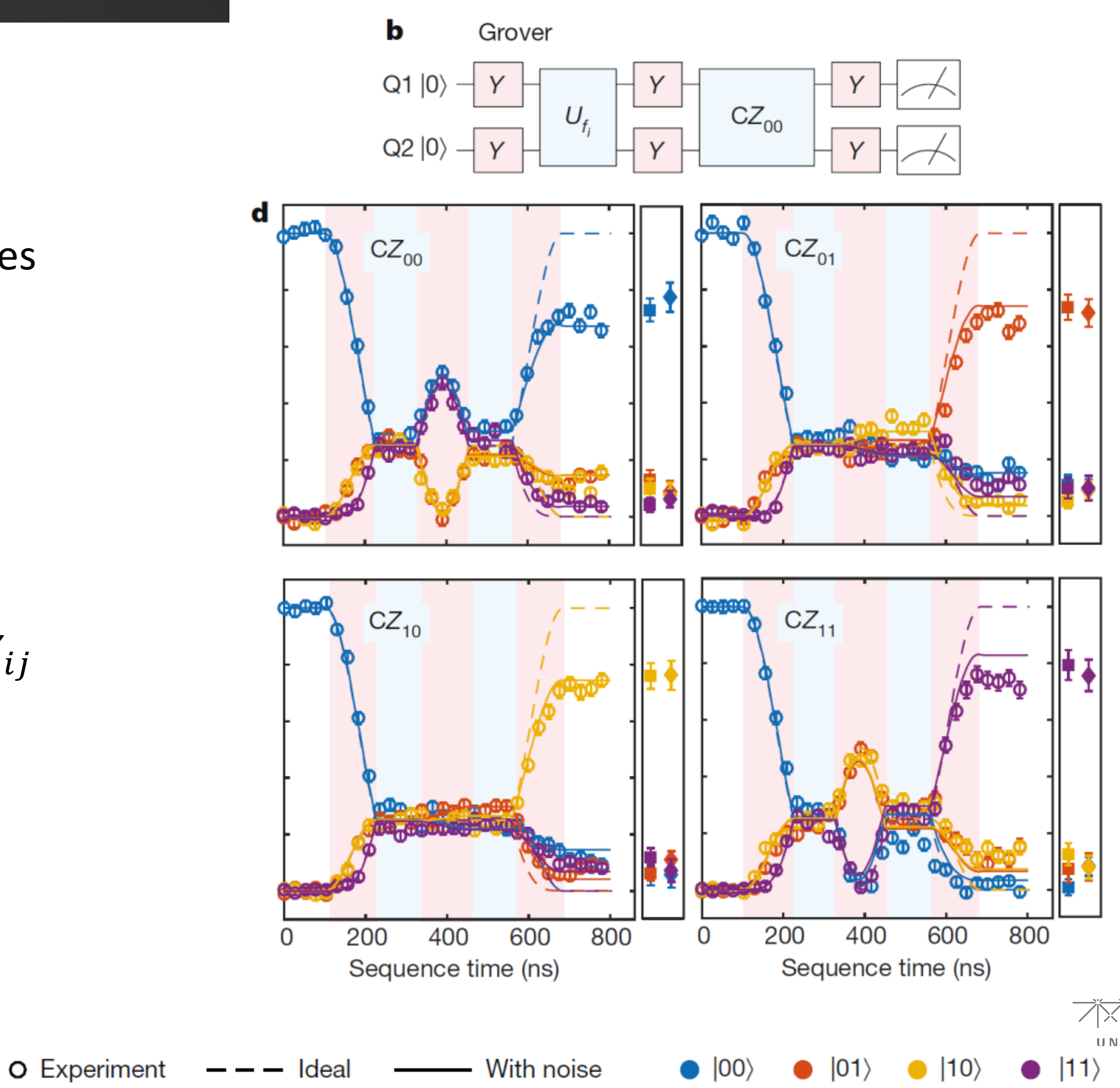

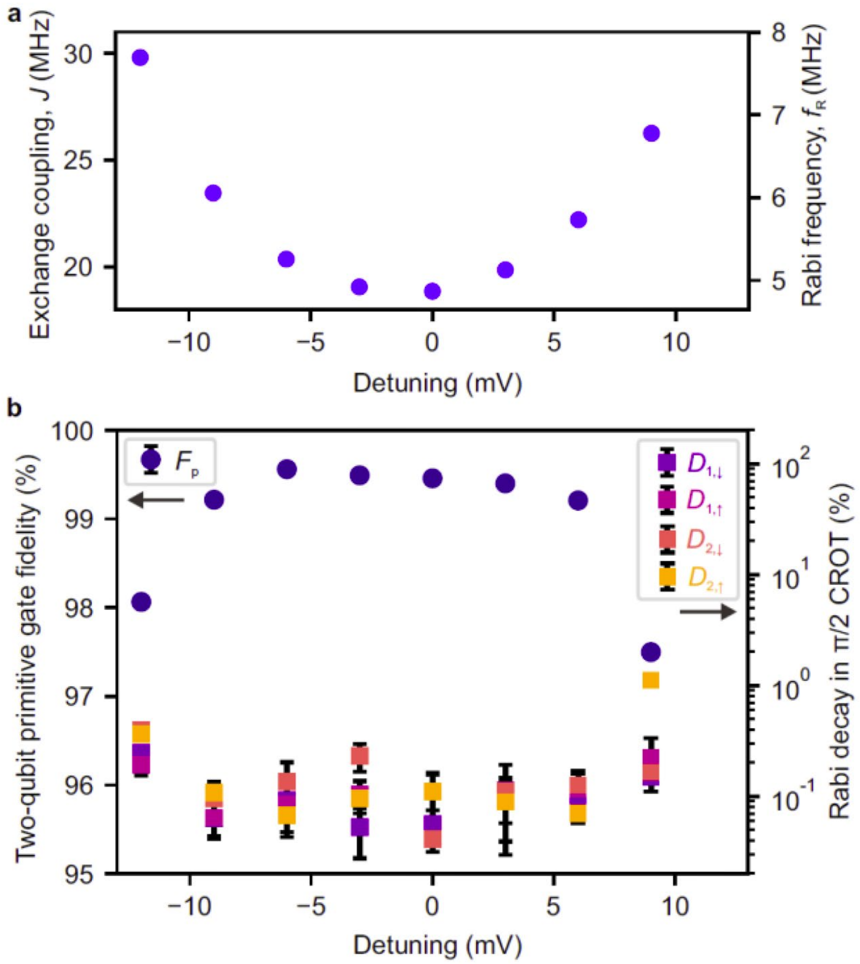
a
Exchange coupling, J (MHz)
Rabi frequency, f_R (MHz)
Detuning (mV)
b
Two-qubit primitive gate fidelity (%)
F_p
$D_{1,\downarrow}$
$D_{1,\uparrow}$
$D_{2,\downarrow}$
$D_{2,\uparrow}$
Rabi decay in π/2 CROT (%)
Detuning (mV)

Two-qubit gate fidelity

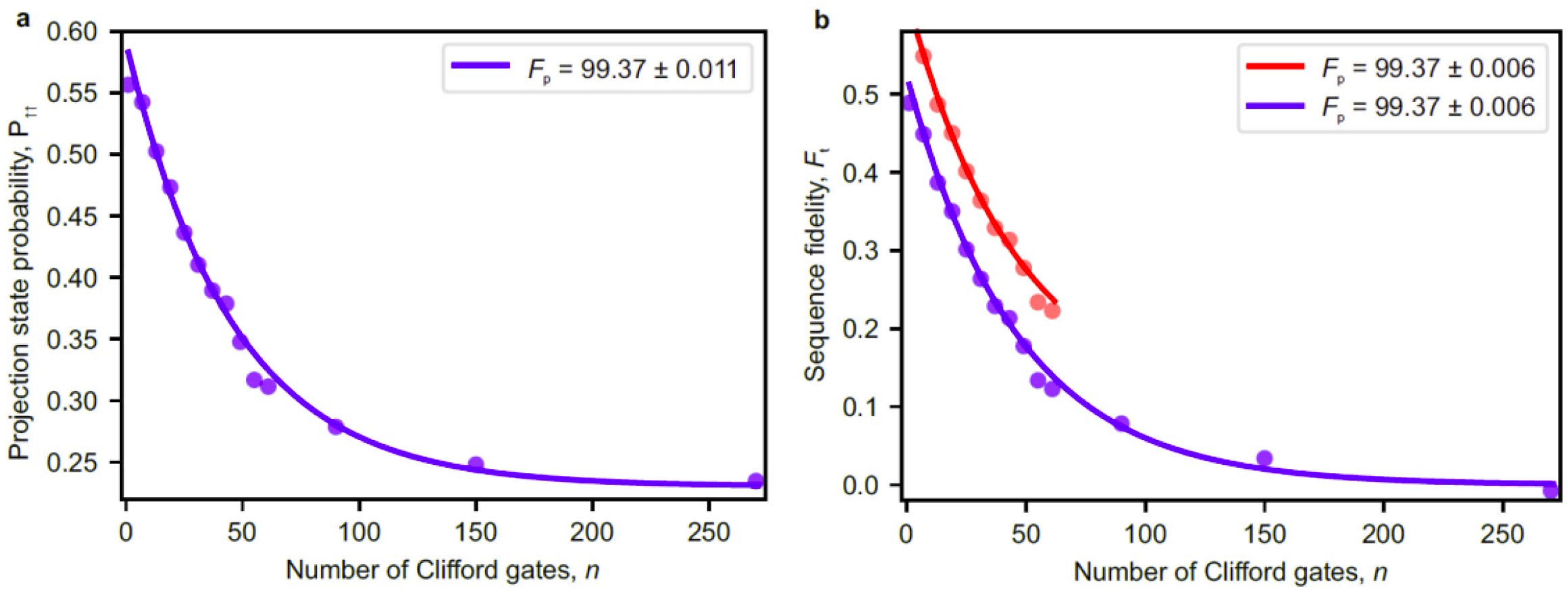

UNI BASEL

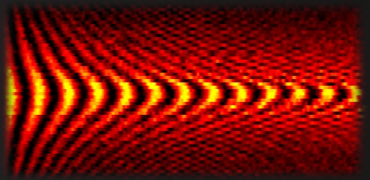

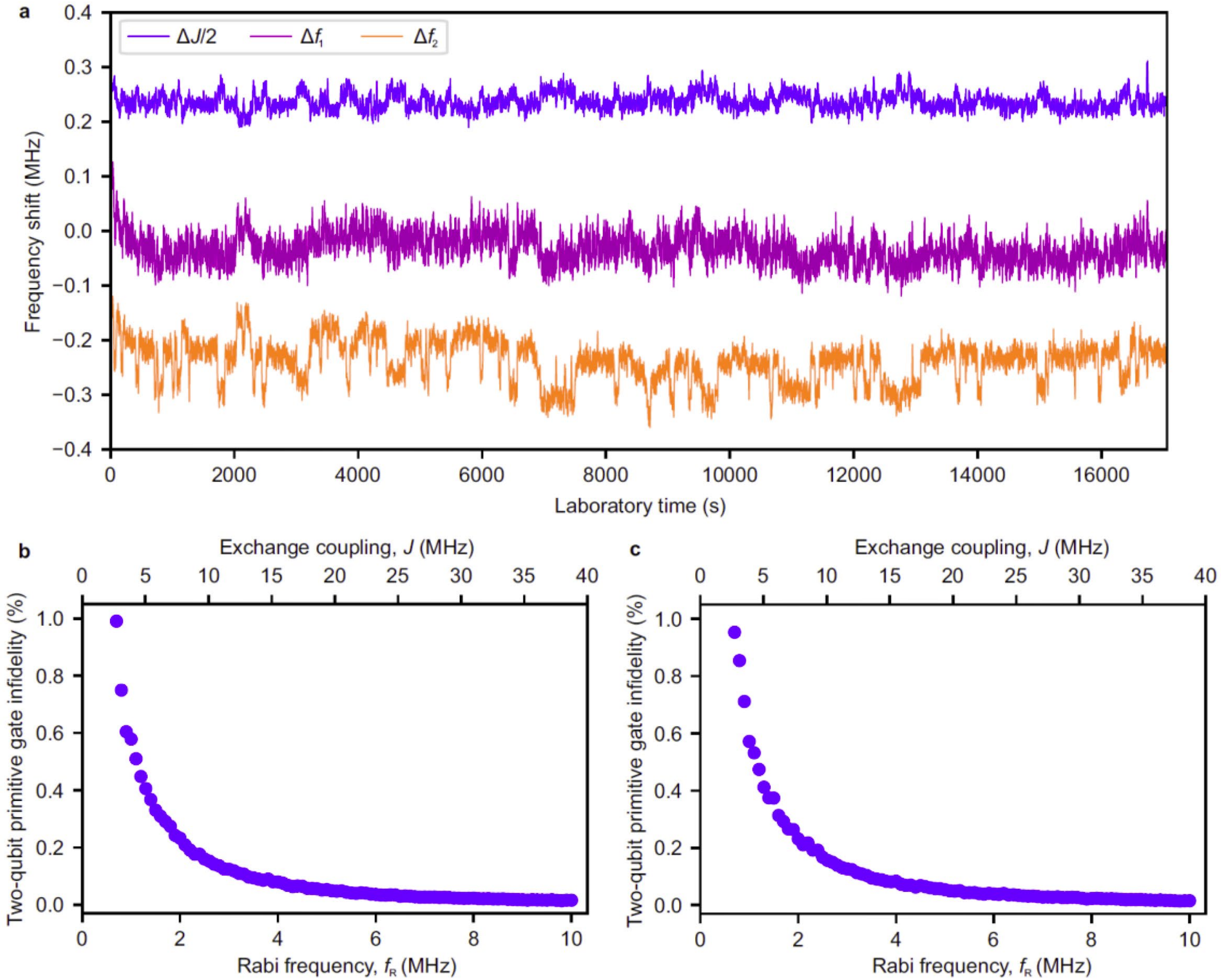

a
ΔJ/2
Δf1
Δf2
Frequency shift (MHz)
0.4
0.3
0.2
0.1
0.0
−0.1
−0.2
−0.3
−0.4
0
2000
4000
6000
8000
10000
12000
14000
16000
Laboratory time (s)
b
c
Exchange coupling, J (MHz)
0
5
10
15
20
25
30
35
40
Two-qubit primitive gate infidelity (%)
1.0
0.8
0.6
0.4
0.2
0.0
0
2
4
6
8
10
Rabi frequency, fR (MHz)

UNI BASEL

Output states of Deutsch-Josza and Grover search algorithm

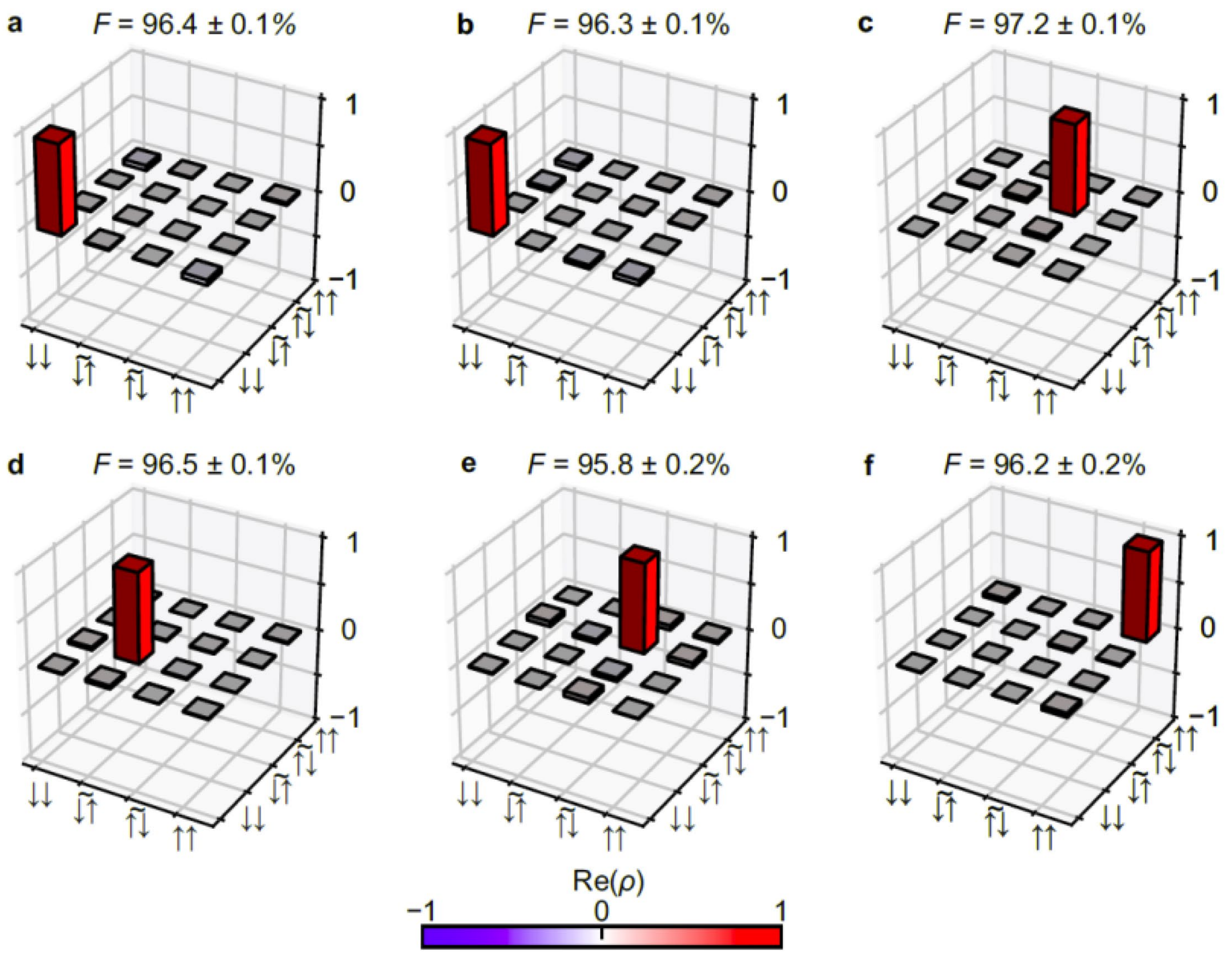

Single Qubit Performance

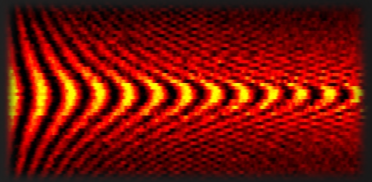

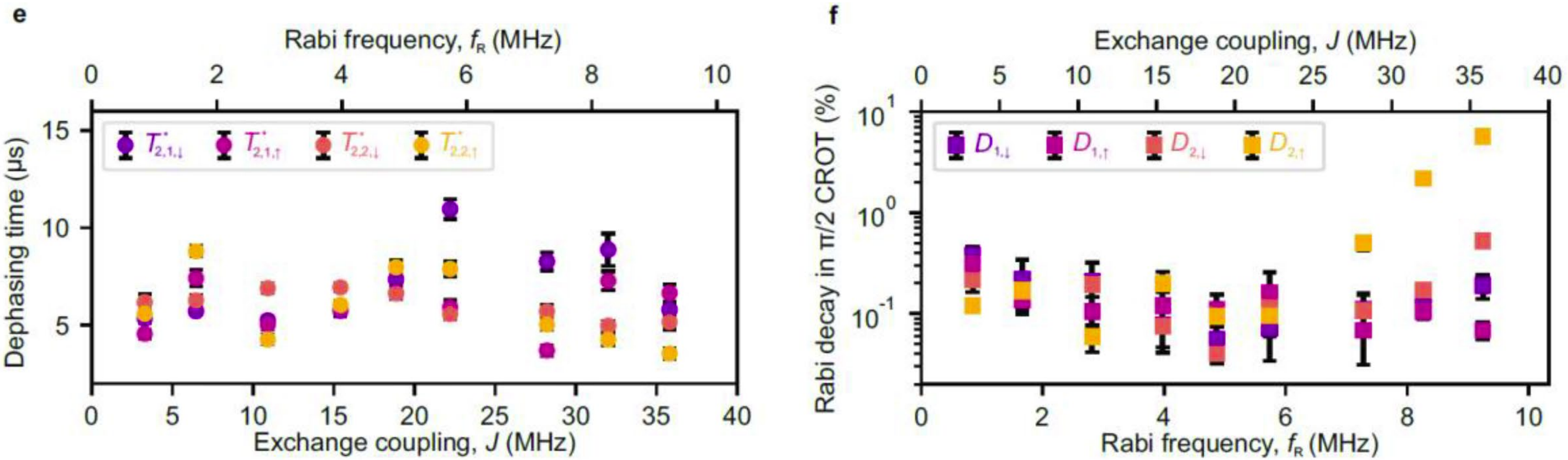

Two-qubit quantum processing

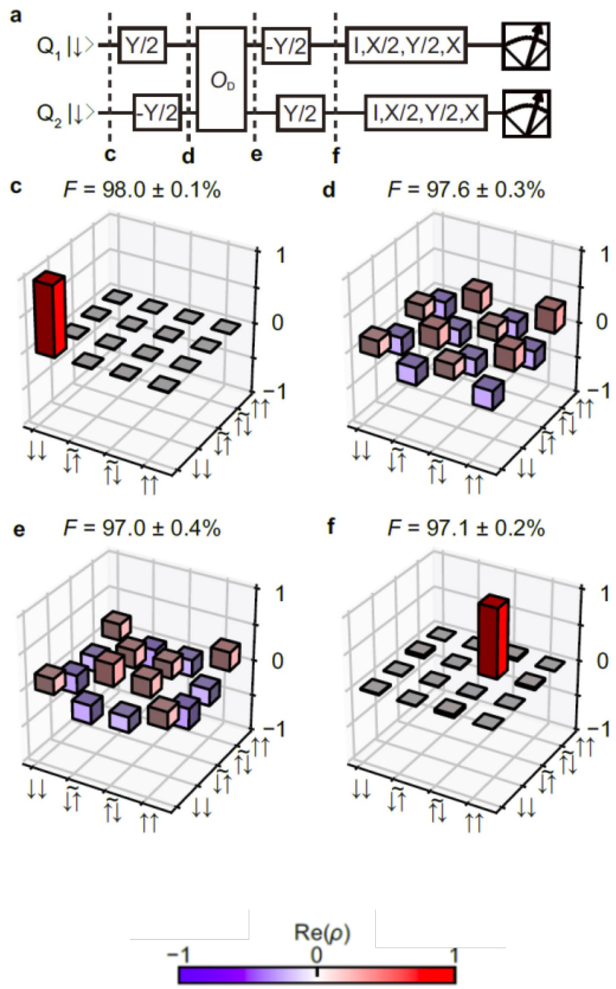

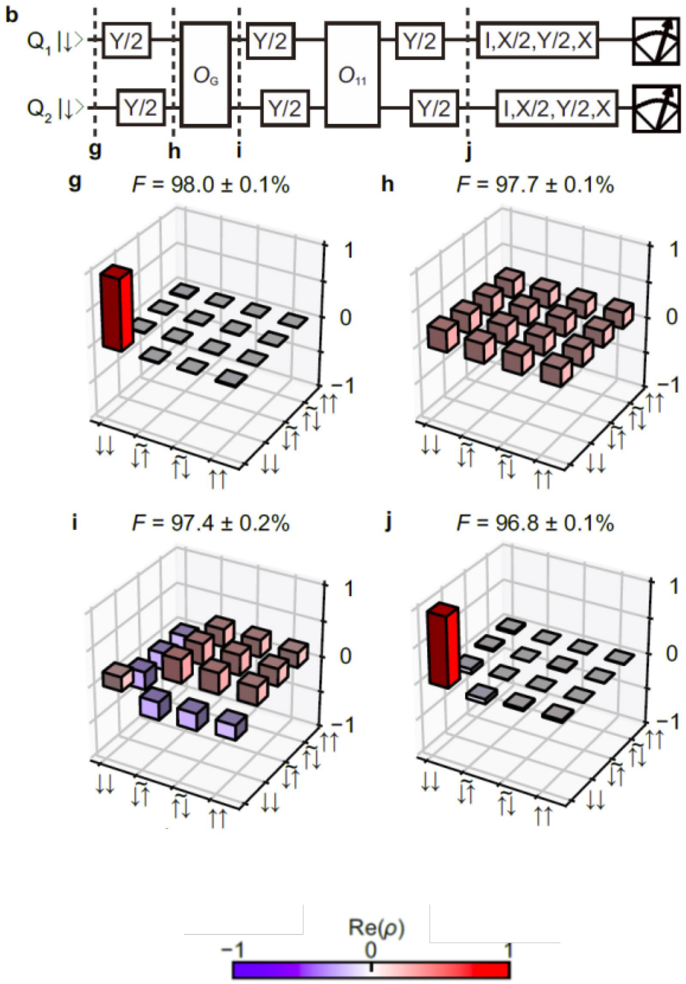
b
Q1 |↓⟩
Q2 |↓⟩
Y/2
O_G
O_{11}
I,X/2,Y/2,X
g
h
i
j
g F = 98.0 ± 0.1%
h F = 97.7 ± 0.1%
i F = 97.4 ± 0.2%
j F = 96.8 ± 0.1%
Re(ρ)
−1
0
1

Two-qubit quantum processing

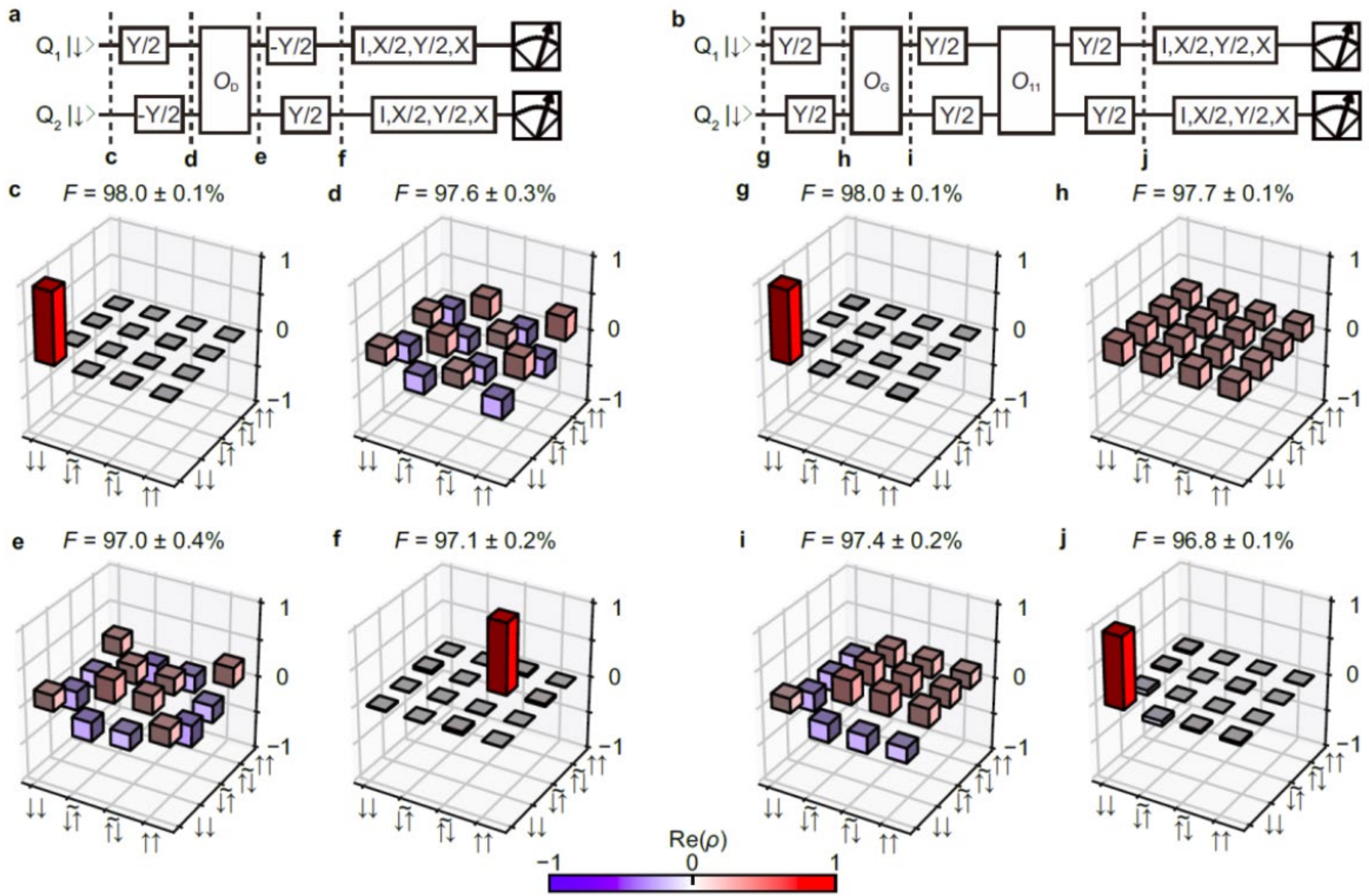

Overview: spin qubit platforms

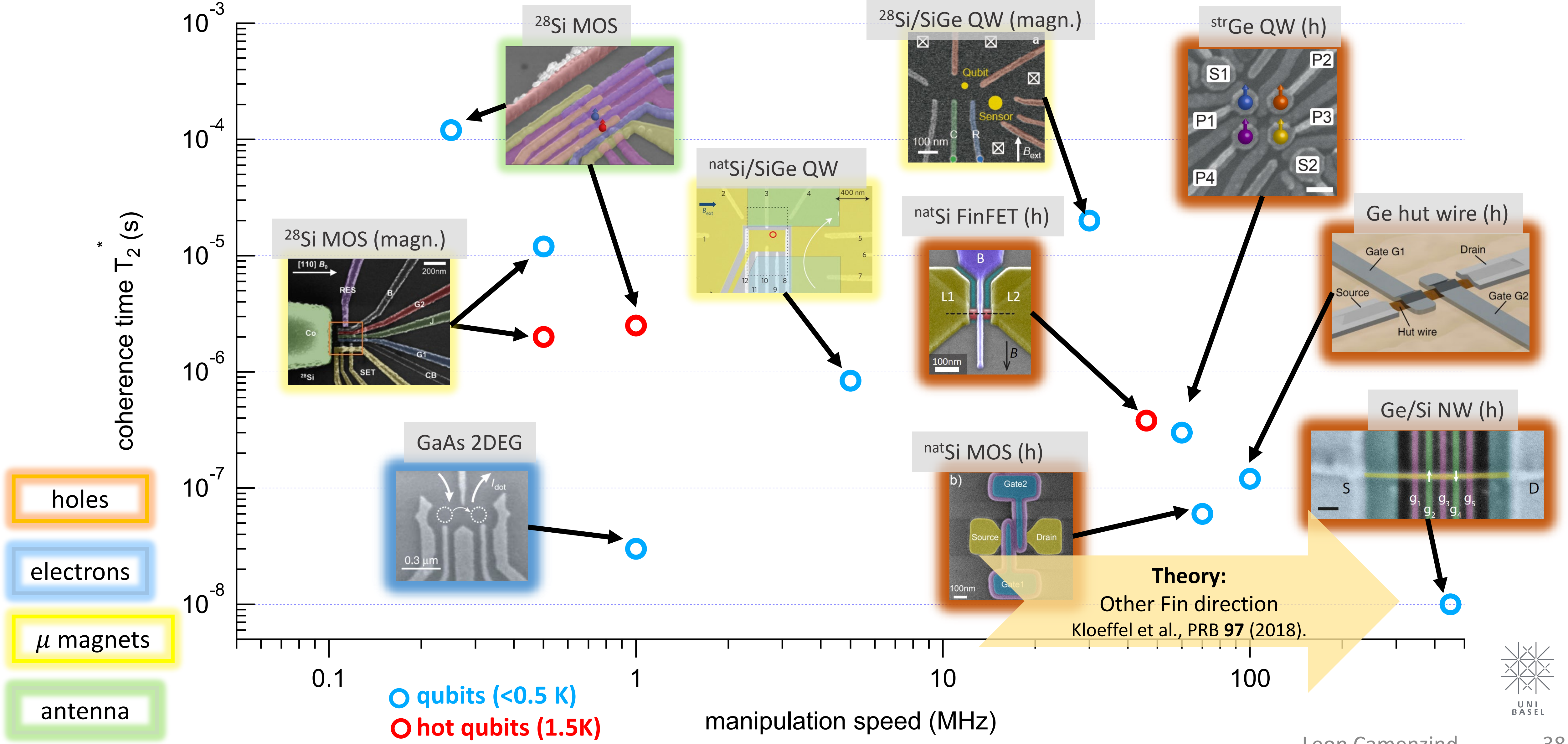

Quality factor Q^*

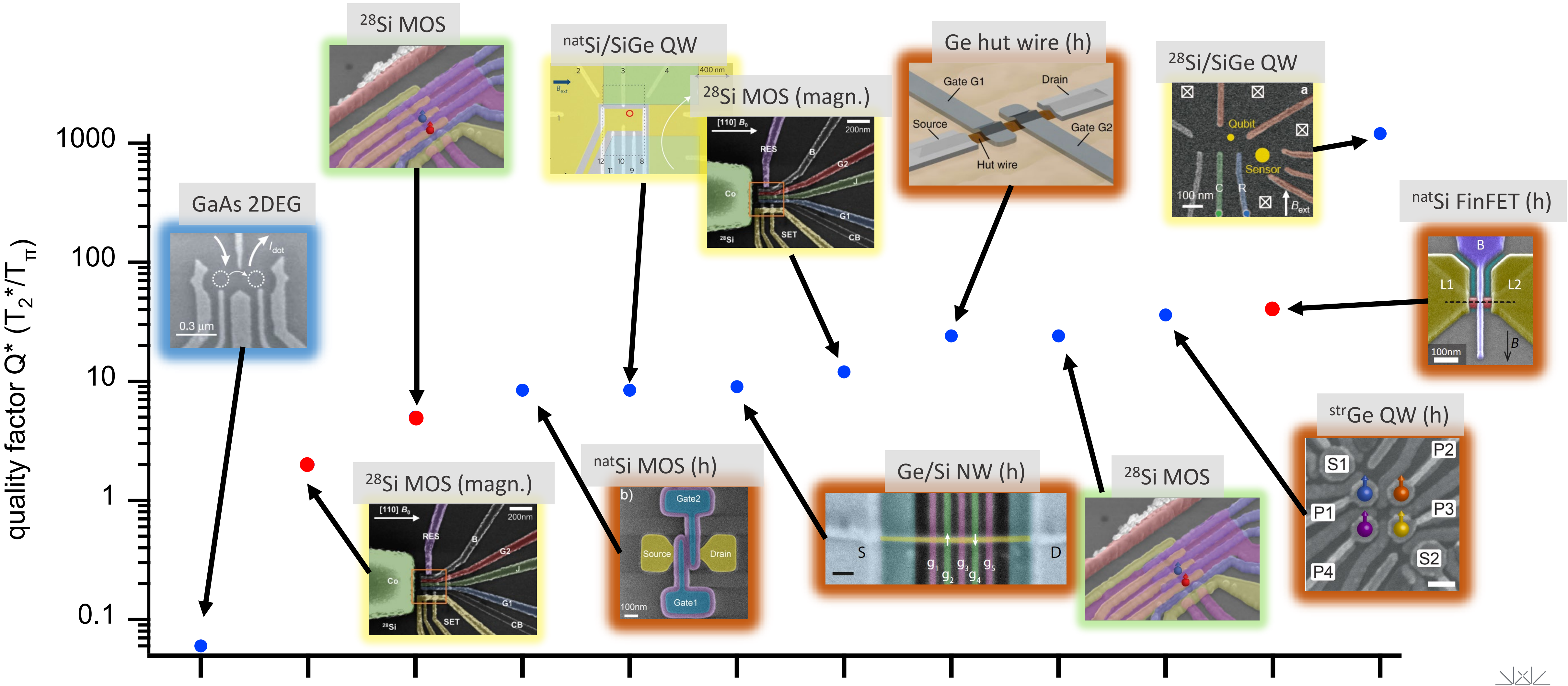

Comparison to Superconducting qubits

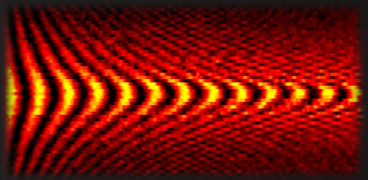

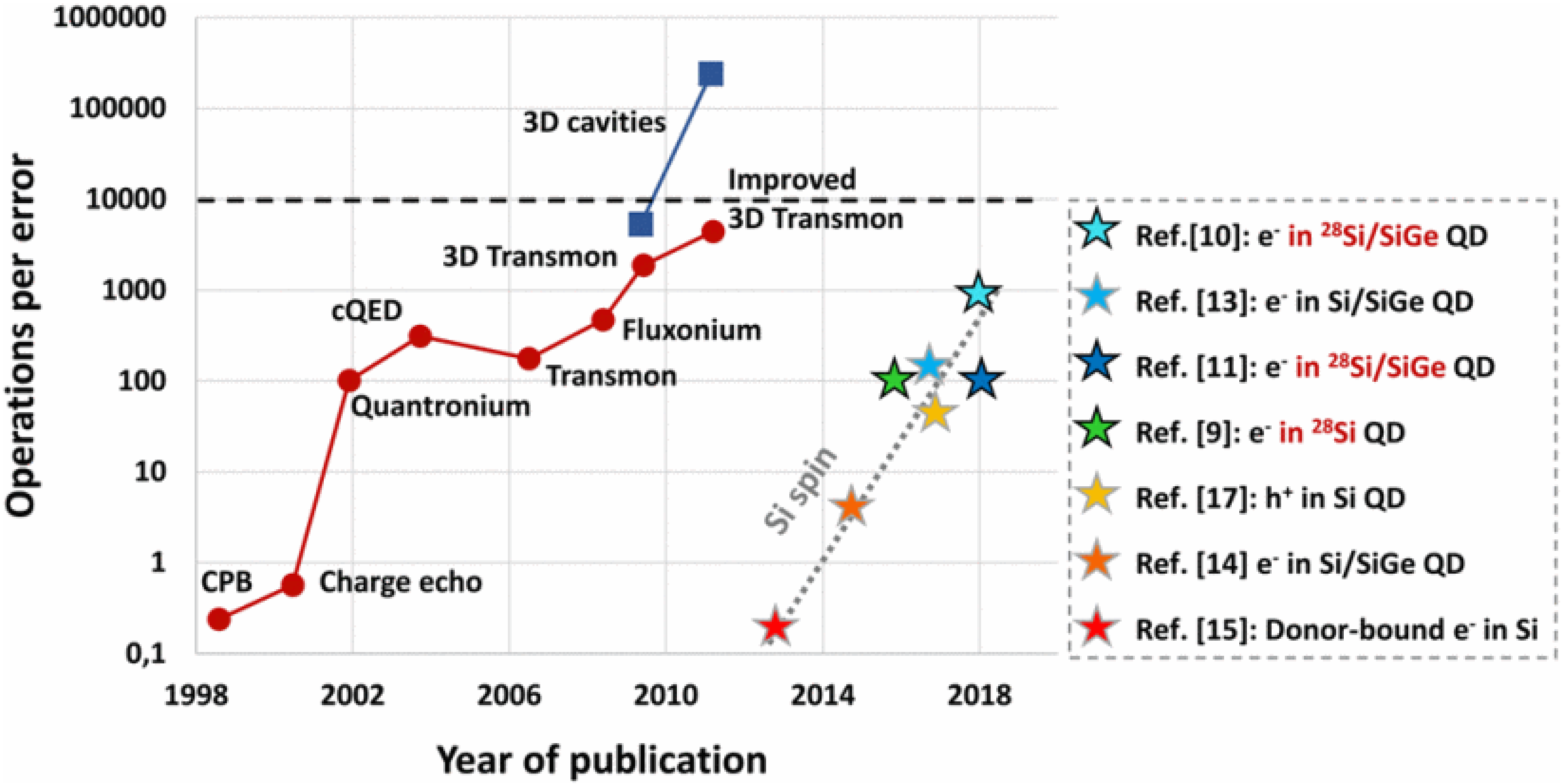

Hutin et al., Si MOS technology for spin-based quantum computing,
48th European Solid-State Device Research Conference (ESSDERC) (2018)

Fault tolerant spin qubits

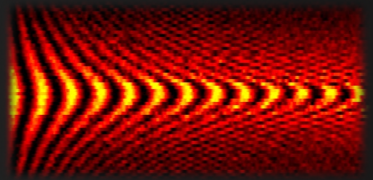

operation	current fidelity	reference
Single-qubit gates	99.93%	Yoneda et al. Nat. Nanotechnol. **13** (2018).
Two-qubit gates CROT	98.0% (RBM)	Huang et al., Nature ***569*** (2019).
Two-qubit gate SWAP	< 90%	Sigillito et al., npj Quant. Inform. **5** (2019).
Elzerman **readout**	< 90%	Keith et al., New J. of Phys. **21** (2019).
QND **readout**	>95%	Nakajima et al., Nat. Nano. **14** (2019).
Initialization	<99% (at 55ms)	Keith et al., New J. of Phys. **21** (2019).

Fault-tolerant qubits:

- F_S (1-qubit) > 99.9%,
- F_{2Q} ***(2-qubit) > 99%***
- F_{init} ***(Initialization) > 99%***
- F_{RO} ***(read-out) > 99%***

Fowler *et al.*, Phys. Rev. A **87** (2009).

^{28}Si/SiGe QW (magn.)

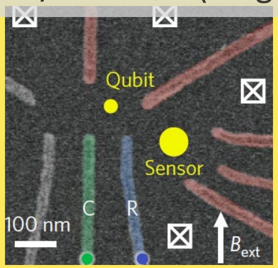

Future Project:
Fault-tolerant silicon qubit systems :
2, 3 and 5 qubits

Appendix II

Spin Qubit control

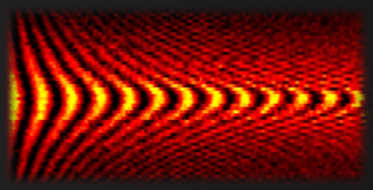

On-chip stripline (f_{Rabi} up to 10 MHz)

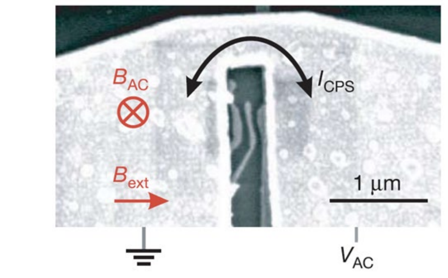

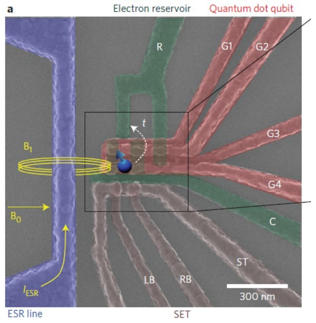

GaAs: Koppens et al., Nature, 442 (2006).

SiCMOS: Veldhorst et al., Nat. Nano, 216 (2014).

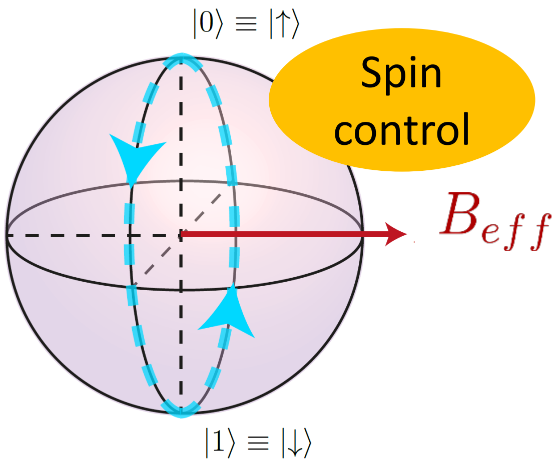

Hyperfine interaction (not coherent)

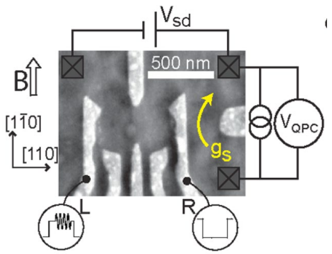

Laird et al, Phys. Rev. Lett. 99, 246601 (2007)

Micromagnets (up to 130 MHz)

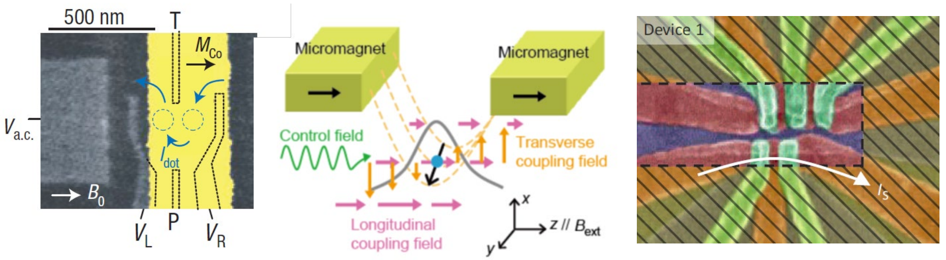

Pioro-Ladrière et al., Nat. Phys. 4, 776-779 (2008).

Kawakami et al., Nat. Nano. 9, 153 (2014).

Yoneda et al., Nat. Nano. 13, 102 (2018).

Borjans et al., Phys. Rev. Appl. 11, 044063 (2019).

spin-orbit interaction (up to 140 MHz)
g-tensor modulation (~40 MHz)

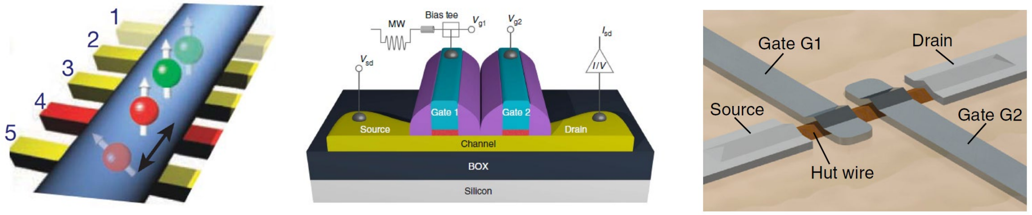

GaAs 2DEG: Nowack et al., Science 318, 1430-1433 (2007).

InAs Nanowire: Nadj-Perge et al., *Nature 468*, 7327 (2010).

Hole SiCMOS: Maurand et al., Nat. Commun., 1357 (2016).

Hole SiCMOS: Crippa et al., Phys. Rev. Lett. 120, 137702 (2018).

Hole in Ge hut wire: Watzinger et al, Nat. Commun. 9, 3902 (2018).

Hole in strained Ge well: Hendrickx et al, Arxiv 1912:10426 (2019).

Comparison: State of the art performance

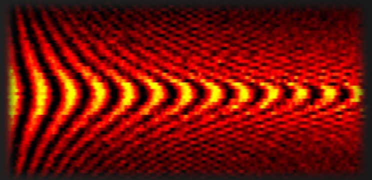

$^{28}Si/SiGe$ QW

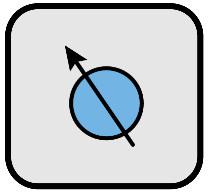

0.06%

Quantum well devices

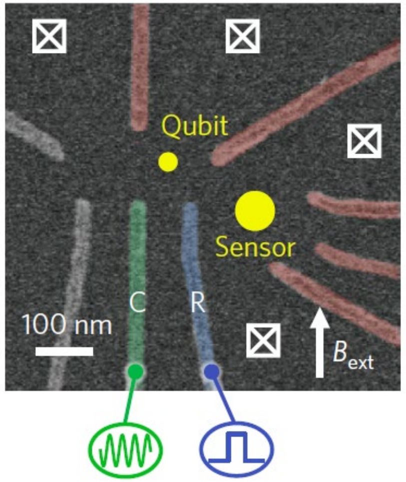

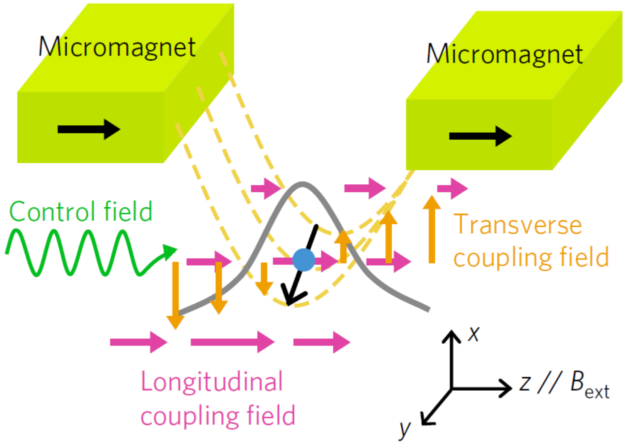

Yoneda et al., Nat. Nano **13**, 102 (2018).

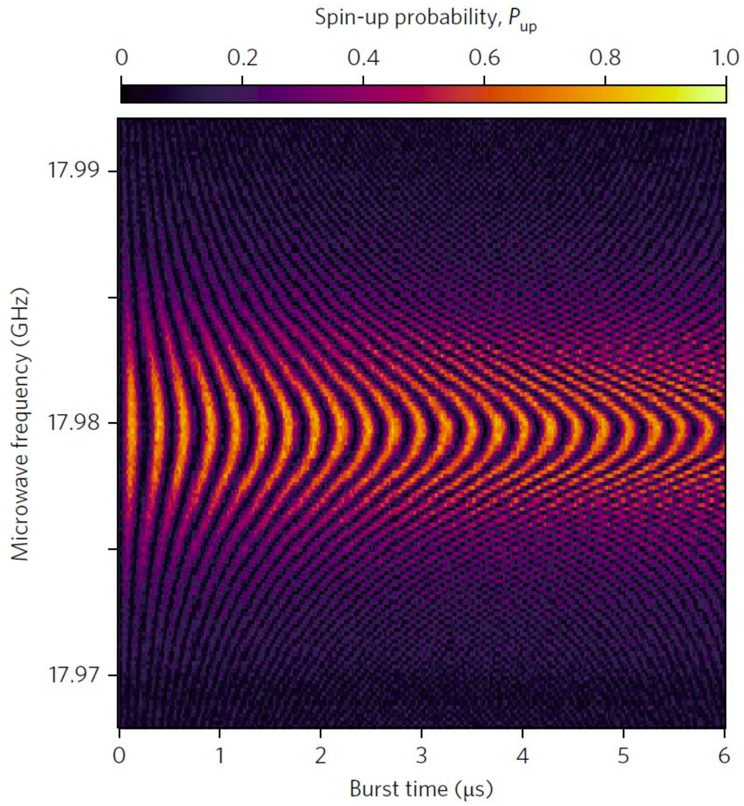

T ≈ 100 mK

f_{Rabi} up to **30 MHz**

$T_2^* = 20\ \mu s$

F_S = **99.926** ± 0.002%.

Bottleneck: Two-qubit gates

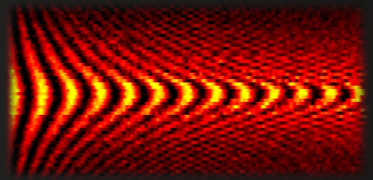

Trade off between dephasing and gate-speed

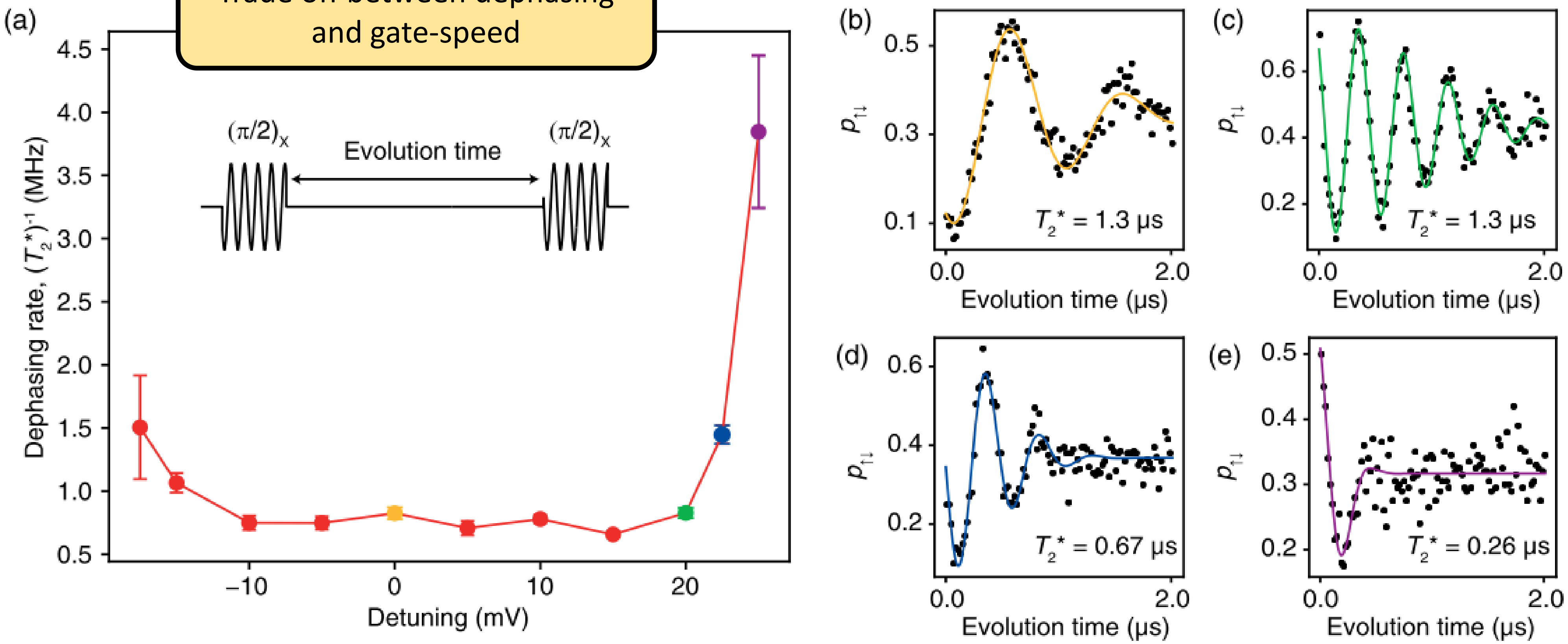

Here S-T Qubit: $F_S = 99.6\%$ limited by nuclear noise.

“The same resonant control technique can be applied to an array of spin-1/2 qubits to implement a SWAP gate..”

Takeda et al., Phys. Rev. Lett. 124, 117701 (2020).